

# **Core Model Proposal #393: Update AgLU parameters for land-based mitigation measures**

**Product:** Global Change Analysis Model (GCAM)

**Institution:** Joint Global Change Research Institute (JGCRI)

**Authors:** Xin Zhao

**Reviewers:** Abigail Snyder and Marshall Wise

**Date committed:** 03/20/2024

**IR document number:** PNNL-ACT-10137

**Related sectors:** Agriculture, Land, and Bioenergy

**Type of development:** Data and Code

**Purpose:** This Core Model Proposal improves GCAM parameters and assumptions related to (1) land allocation (e.g., primarily a lower logit exponent to enhance behavior), (2) the implementation of land carbon pricing policy, (3) food demand (allowing for price-induced dietary changes), and (4) the supply and trade of primary biomass. Most of the changes were suggested by recent GCAM studies that focused on agroeconomic projections or land-based mitigation measures (e.g., universal land carbon tax, afforestation/reforestation, and bioenergy in combination with carbon capture and sequestration). We document the changes and provide the related modeling details. With these changes, agroeconomic projections related to land allocation, dietary changes, agricultural and food prices, land use change emissions, and land-based mitigation policy implications are improved.

## Contents

1. Introduction .....	2
2. Key areas of improvement and description of changes.....	2
2.1. Logit land allocation and parameter updates .....	2
Fig. 1 Land nesting structure in GCAM.....	4
2.2. Land rental profit and shadow rental profit for unmanaged land updates .....	4
2.3. Update the social discount rate in the land system mitigation policy assumptions .....	5
2.4. Update land carbon policy implementation assumption (adding minimum soil carbon density) .	6
2.5. Agricultural demand responses.....	7
Fig. 2 Food demand nesting structure in GCAM.....	8
2.6. Residual biomass supply curve.....	8
2.7. Other updates in assumptions driving biomass market expansion.....	8
Fig. 3 Schematic of biomass flows in GCAM.....	9
2.8. Overview of key changes in gcamdata .....	1
Table 1 key data and code changes made in gcamdata .....	1
3. Shared policy assumption (SPA) GCAM validation runs.....	2
Fig. 4 Global and regional changes in cumulative carbon dioxide emissions in 2020 - 2100. ....	4
Fig. 5 Cumulative carbon dioxide emissions (starting 2020).....	5
Fig. 6 Global net carbon uptakes in terrestrial and ocean systems and atmosphere carbon concentration.....	6
Fig. 7 Forcing, mean temperature change, and carbon prices.....	7
Fig. 8 Global land use change.....	8
Fig. 9 Global cropland change.....	9
Fig. 10 Global primary biomass supply by source.....	10
Fig. 11 Global residual biomass supply by source.....	11
Fig. 12 Global biomass demand by source.....	12
Fig. 13 Global food calorie consumption supply by source.....	13
Fig. 14 Global agricultural prices by sector.....	14
Fig. 15 Global fertilizer consumption changes.....	15
Fig. 16 Global water withdrawal changes by sector.....	16
Fig. 17 Global GHG (CO <sub>2</sub> , CH <sub>4</sub> , and N <sub>2</sub> O) emissions.....	17
4. Summary and future work.....	18
Supplementary Information .....	20
References.....	25

## 1. Introduction

Robust global economic and multisector dynamic modeling hinges on the quality of assumptions governing data and parameters which are crucial representations of agent (producers and consumers) behaviors. This is particularly the case for Agricultural and Land Use (AgLU) modeling within the framework of GCAM. In a recent study conducted by Zhao et al. (2024b), there was a significant update to GCAM AgLU parameters, specifically addressing the exploration of land-based mitigation measures, such as afforestation/reforestation (or land carbon storage policies) and bioenergy with carbon capture and sequestration (BECCS), and the corresponding economic and environmental implications, e.g., agricultural prices. Model projections aligned more closely with existing literature with the updates.

Building upon this recent advancement, the present Core Model Proposal (CMP) focuses on refining GCAM parameters and assumptions critical to AgLU modeling. The main areas include (1) improving land allocation through adjustments like a lower logit exponent to improve behavioral representation, (2) refining the implementation of land carbon pricing policies, (3) accommodating price-induced dietary changes to enhance the accuracy of food demand modeling, and (4) fine-tuning the modeling of the supply (mainly residues) and trade dynamics of primary biomass. The theoretical background and technical details of these changes are documented. Most of the changes proposed make the modeling more flexible. With these changes, agro-economic projections related to land allocation, dietary changes, agricultural and food prices, land use change emissions, and land-based mitigation policy implications are improved.

## 2. Key areas of improvement and description of changes

### 2.1. Logit land allocation and parameter updates

Land allocation in GCAM is modeled using the nested logit approach (Wise et al., 2014), in which landowners in a water-economy region allocate land across uses to maximize a preference-adjusted rental profit (Zhao et al., 2020a), subject to physical area constraints and unconditional rental profit distribution that is determined by cost and land productivity information. The derived logit land share in a nest for land  $i$  is  $S_i$ , which is a function of logit share-weights ( $\alpha_i$ ), logit exponent ( $\theta$ ), and rental profits ( $r_i$ ).

$$S_i = \frac{\alpha_i r_i^\theta}{\sum_j \alpha_j r_j^\theta} \quad (1)$$

The land sharing maintains physical land balance in a nest, i.e.,  $\sum_j S_i = 1$ , and land competes grossly based on rental profits. While transition-based land use modeling approaches were tested in previous studies, they either relied heavily on assumptions or data not widely exist, e.g., transition function in Ferreira Filho et al. (2015), or did not consider economic responses, e.g., the Markov model in Li and Wu (2022). The logit land allocation method is parsimonious,

flexible in nesting structure, and connects biophysical information to economic behavior (Fujimori et al., 2014; Taheripour et al., 2020; Wise et al., 2014; Zhao et al., 2020a, 2020b). The land nesting structure used in GCAM is shown in **Fig. 1**. Note that purpose-grown energy croplands are introduced in 2025 in GCAM by gradually phasing in their share-weights in the logit nesting structure.

GCAM includes all land data in the base year, as compiled and processed by its designated open-source Moirai land data system (Di Vittorio et al., 2020). Prior to GCAM v6, the default land data assumption in GCAM was that 90% of natural ecosystems are protected (Calvin et al., 2019). This implies that 90% of unmanaged forest, unmanaged pasture, grassland, and shrubland were assumed to remain undisturbed in future land reallocation. The assumption results in a rigid natural land supply elasticity because the logit approach depends on both the logit exponent parameters and historical land allocation to determine land supply elasticity. Recently, in GCAM v6 (CMP-329), the natural land availability assumption was updated based on regional land availability data compiled in Moirai (Narayan et al., 2022). The new data indicates that about 30% of the natural land globally is unavailable due to land conservation policies (IUCN, 2018) or unsuitability (Zabel et al., 2014). As tested and demonstrated in Di Vittorio et al. (2023), land availability assumptions could have critical implications on regional land projections. However, it is important to note that when lowering natural land availability in the base data, it effectively increases the corresponding land supply elasticities. **Thus, in this CMP, we recalibrate the land logit exponent parameters to ensure that the own-price natural land supply elasticity remains comparable to the original GCAM assumptions.** The recalibration resulted in more rigid land supply elasticities, more consistent with the broader literature (Ahmed et al., 2008). The key land logit exponent parameters are now  $\theta^{Arable} = 1.75$ ,  $\theta^{Pas} = 2$ ,  $\theta^{NonPas} = 0.75$ , and  $\theta^{For} = 1.25$  (**Fig. 1**). These values are mostly lower than the previous ones used in GCAM, which were  $\theta^{Arable} = 2$ ,  $\theta^{Pas} = 3$ ,  $\theta^{NonPas} = 1.25$ , and  $\theta^{For} = 1.75$ .

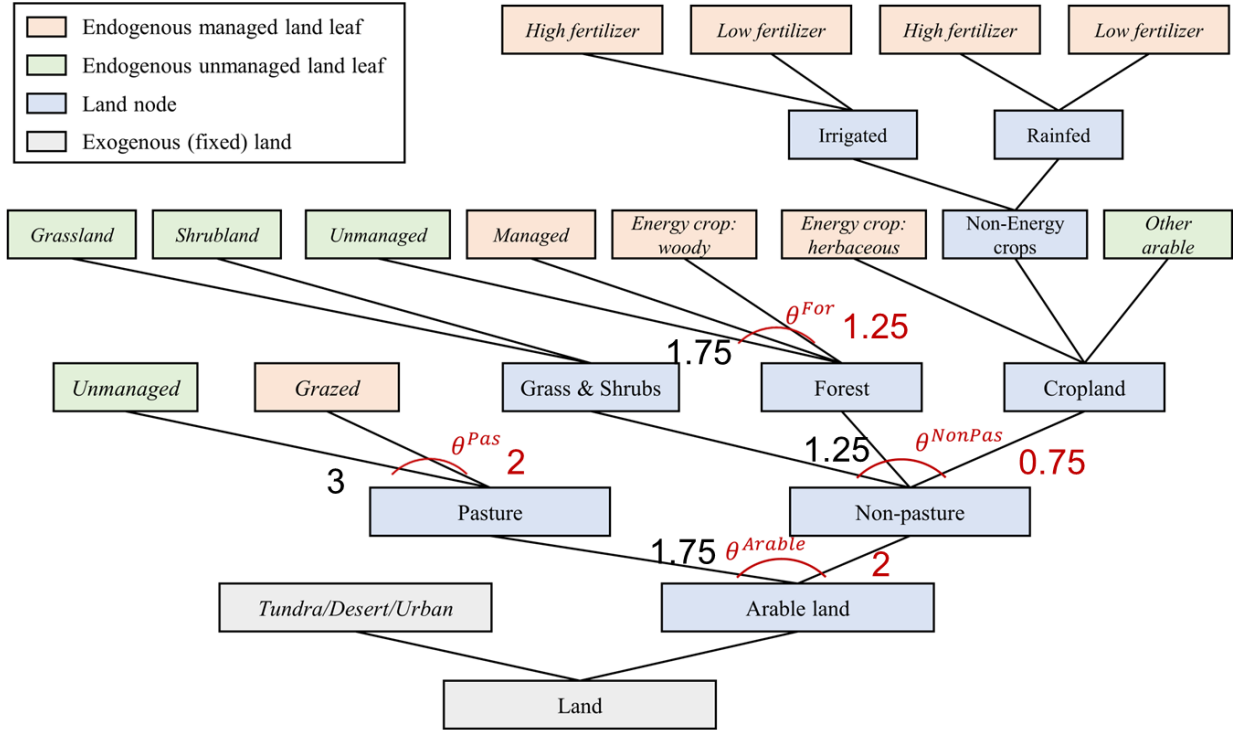


Fig. 1 Land nesting structure in GCAM. The set of key logit exponent parameters proposed in this CMP is  $\theta^{Arable} = 1.75$ ,  $\theta^{Pas} = 2$ ,  $\theta^{NonPas} = 0.75$ , and  $\theta^{For} = 1.25$  (proposed values in red and original values in black). Note that managed (grazed) pasture is used in the Beef, Dairy, and Sheep & Goat sectors in GCAM. In addition, like non-energy crops, energy crop production technologies in GCAM are also differentiated by irrigation and fertilizer use. The other arable land corresponds to “land with temporary fallow” in FAOSTAT land data. In addition, in a recent CMP, forest land was also separated into hardwood and softwood.

## 2.2. Land rental profit and shadow rental profit for unmanaged land updates

Agricultural production is modeled using the Leontief production function, and endogenous yield responses in crop production are realized via technology switching, e.g., fertilizer and irrigation options. Given the profit-maximizing agricultural producers and constant-return-to-scale (CRTS) production functions, the rental profit,  $r_i$ , can be derived for managed land, i.e., land with economic activities (Eq. 2).

$$r_i = (p_i - NLC_i) \cdot g_i \quad (2)$$

Note that  $p_i$  is market prices,  $g_i$  is yield, and  $NLC_i$  is nonland costs (e.g., water, fertilizer, and others) per unit of output. And the shadow profit of unmanaged land is determined by the derived rental profit of managed land in base data. The production of forestry products in GCAM also uses the Leontief production function with the productivity coefficients connecting the primary roundwood production and managed forest land cover. Forestry data from FAOSTAT is

used, and the cost share data from the GTAP v10 database is used. The forestry rental profit can also be calculated using **Eq. 2**.

There is no observed rental profit for unmanaged land since it is not currently being used for economic activities. However, the shadow price of unmanaged land, e.g., implying a marginal cost of land conversion or an ecosystem service value, is an important factor determining the supply curve of unmanaged land. GCAM relies on a land dataset compiled by the Center for Sustainability and the Global Environment (SAGE) and the Global Trade and Analysis Project (GTAP) (Ramankutty et al., 2005) for estimating the shadow price of unmanaged land. It is calculated as the average land rental profit across managed land in a region (water basin). For example, the global mean value is \$140 per ha. In contrast, this value calculated using GCAM data would be about 30% higher (\$190 per ha). **In this CMP, we update the unmanaged land value to use the ones directly computed based on GCAM data since it is more consistent and avoids potential aggregation uncertainties in processing SAGE-GTAP data.** In the new data, the median value across all regions is \$143 per ha, and the 5<sup>th</sup> to 95<sup>th</sup> percentile range is \$38 to \$475 per ha. This update has a more significant impact on the distribution's shape and tails. In general, unmanaged land supply (e.g., afforestation/reforestation and deforestation) becomes less sensitive to land policies due to higher overall shadow prices of unmanaged land. Note that the changes in land rental prices will affect the initial calibration of the share-weights in the logit function used for land allocation, implying different landowner's preferences.

The calculation of the unmanaged land rental profit is added to the chunk ``input/gcamdata/R/zaglu_L221.land_input_1.R``. Currently, we kept the ability of using the original method (when `UsingGCAMCroplandRentalProfit = F` in the Chunk).

### 2.3. Update the social discount rate in the land system mitigation policy assumptions

The land system mitigation policy in GCAM is implemented as a carbon rent, i.e., land subsidy, to credit landowners for holding carbon stocks. The approach is consistent with the nested logit land allocation method used in GCAM. As shown in **Sections 2.1** and **2.2**, land allocation is initially calibrated to historical data, and the relative land use (or land share) is responsive to relative land rental profit. With land system mitigation policies, carbon stored in land will be valued. That is, the land rental profit is increased to  $r'_i$  when factoring in an annualized land carbon storage rent,  $d_i$  (**Eq. 3**). And  $d_i$  is a product of the social discount rate ( $\eta$ ) and the net present value (NPV) of carbon storage in both vegetation ( $NPV_i^{veg}$ ) and soil ( $NPV_i^{soil}$ ) (**Eq. 4**).

$$r'_i = r_i + d_i \quad (3)$$

$$d_i = \eta \cdot (NPV_i^{veg} + NPV_i^{soil}) \quad (4)$$

**In this CMP, we update the social discount rate from  $\eta = 2\%$  to  $\eta = 3\%$ , to be more consistent with the Hotelling rate used to determine the carbon price escalation rate.** The

change was made in `cvs/objects/containers/source/region_minicam.cpp` (`DEFAULT_SOCIAL_DISCOUNT_RATE = 0.03`). Note that land carbon policy implications are highly sensitive to the social discount rate. The land carbon subsidy (annuity) would increase by 50% with this change. As indicated in Eq. 4, this change will increase the land carbon subsidy and, consequentially, land carbon pricing policies will be more effective.

#### 2.4. Update land carbon policy implementation assumption (adding minimum soil carbon density)

GCAM specifies carbon density at the equilibrium state, i.e., the maximum potentially achievable carbon density for a given land leaf, for vegetation carbon density ( $CD_i^{veg}$ ) and soil carbon density ( $CD_i^{soil}$ ). However, accounting for the dynamics of land carbon changes is essential, given the nonlinear nature of plant growth and soil carbon change. In GCAM, when the land area expands, the vegetation carbon growth follows a sigmoid function of the “mature-year” that is region- and land-specific, while vegetation carbon is released immediately (within a 5-year model step) for decreasing area. For both increases and decreases, the soil carbon changes follow an exponential function with a half-life implied by the regional “soil-time.”

Thus, for vegetation carbon, the NPV is calculated as an integral of the discounted future carbon flow valued at the land system carbon prices ( $\beta^{Land}$ ), as shown in **Eq. 5**, whereas  $f^{sigmoid}(\cdot)$  is a sigmoid function and  $\mu_t$  are discount factors calculated with a 10% private discount rate. The corresponding NPV equation for soil carbon is presented in **Eq. 6**, whereas  $f^{exponential}(\cdot)$  is an exponential function and  $MCD^{soil}$  is a threshold of a minimum soil carbon density. That is, only the net soil carbon density ( $CD_i^{soil} - MCD^{soil}$ ) is valued for soil carbon to reflect carbon storage that is additional.

$$NPV_i^{veg} = \int_{t=0}^{MatureYear_i} [\beta^{Land} \cdot CD_i^{veg} \cdot f^{sigmoid}(MatureYear_i)_t \cdot \mu_t] \quad (5)$$

$$NPV_i^{soil} = \int_{t=0}^{SoilTime_i} [\beta^{Land} \cdot (CD_i^{soil} - MCD^{soil}) \cdot f^{exponential}(SoilTime)_t \cdot \mu_t] \quad (6)$$

The detailed land carbon data and parameters can be found in the open-source R package, `gcamdata` (e.g., `/inst/extdata/aglu/LDS/` and `/inst/extdata/aglu/Various_CarbonData_LTsage.csv`).

Previously,  $MCD^{soil} = 0$ , and, in this CMP, we propose to set  $MCD^{soil} = CD_{cropland}^{soil}$ . In particular, we modified the `add_carbon_info()` function in `module-helpers.R` to add an option (“`Min_Soil_C_at_Cropland = TRUE`”).

Our approach to implementing a land carbon rent policy is generally consistent with the theoretical studies that focused on pricing forest carbon (Hashida and Lewis, 2019; Lintunen et al., 2016; Tahvonon and Rautiainen, 2017). The approach allows systemically valuing carbon in

all land types using the same carbon prices and the land carbon price ( $\beta^{Land}$ ) can be linked to carbon prices in the Energy and Industrial Processes sectors.

When land carbon price increases, relative rental profits are affected so that landowners are incentivized to convert low-carbon-density land to relatively higher-carbon-density land. In practice, the effectiveness or responsiveness of land system mitigation policies depends on several key factors: (1) land logit exponents and calibrated logit share-weights, (2) land carbon density accounting method and related parameters (e.g., discount rate, timing parameters, etc.), and (3) initial land allocation data and implied rental profits. For example, when the land logit exponent is small or land availability is limited (e.g., low accessibility), implying a relatively inelastic land supply response, a higher carbon price is required to encourage the same land conversion (e.g., afforestation). Also, land policies tend to be more effective when the carbon densities are more different across land categories since relative rental profits would thus be more sensitive to carbon prices. If all land categories have a similar carbon storage ability, then land mitigation policy would have little impact on carbon storage. Overall, rental profits, as calculated based on production technology specifications and market information, connect land competition and the land mitigation policy to other market-mediated responses.

## 2.5. Agricultural demand responses

In GCAM, a nesting structure (**Fig. 2**) is used to aggregate food from different sources (measured by calories). At the top level (Staples vs. Non-Staples), the approach developed by Edmonds et al. (2017) is used to specify how own- and cross-price elasticities and income elasticities change endogenously with income. In other words, the per capita food calorie consumption is responsive to price & income and substitution is allowed between staple and non-staple food calories, as implied by the parameters specified. Food calories, or dietary energy available, were derived based on food demand (in tonnes) and the conversion factors were compiled based on FAOSTAT data using the R package *gcamfaostat* (Zhao et al., 2024a).

Currently in GCAM, food consumption at the lower nests does not allow substitutions, despite a nested logit structure (i.e., zero logit exponent parameters). That is, calorie consumption share across commodity sources is fixed under Staples or Non-Staples. However, in this CMP, **we allow a more flexible food demand substitution to reflect the endogenous price-induced dietary change**. In particular, we set the logit exponent parameter to -0.25 in all nests (except the top nest) to allow food price induced dietary changes<sup>1</sup>. In mitigation scenarios, GCAM captures the price transmission from the carbon market to the food market. A higher elasticity of substitution in food consumption allows consumers to mediate the food price impacts via more responsive price-induced dietary changes.

---

<sup>1</sup> Note that similar modifications enabling greater flexibility in substitution on the demand side have been tested and implemented in recent studies, e.g., a logit exponent of -0.25 was used in Zhao et al. (2021).

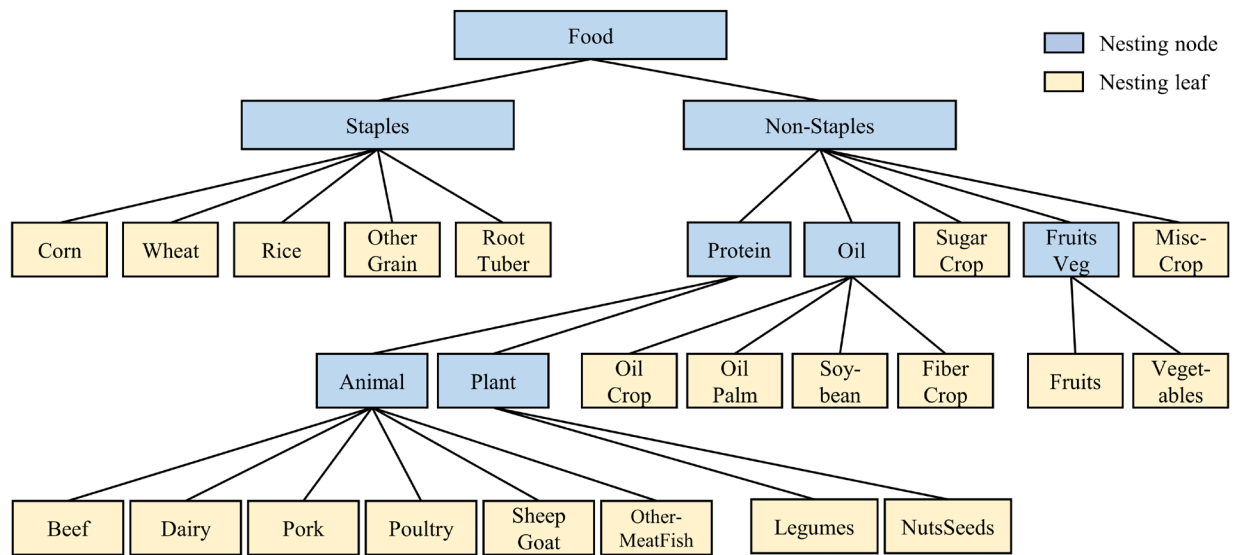


Fig. 2 Food demand nesting structure in GCAM. Note that in this CMP, FiberCrop is moved to the Oil nest since over 99% of the FiberCrop for food consumption is cottonseed oil.

## 2.6. Residual biomass supply curve

The supply curves for agricultural and forestry residual biomass in GCAM were developed based on Gregg and Smith (2010) (Gregg and Smith, 2010). The maximum residual biomass energy availability is derived based on a set of agricultural product-specific attributes, e.g., harvest index, root-to-shoot ratio, water content, energy content, and retention requirement for erosion control. And the maximum availability is endogenously linked to agricultural and forestry production in GCAM, and the share of the availability is responsive to biomass prices. The recent model intercomparison in Hanssen et al. (2020) indicated that GCAM’s residual biomass production is at the high end compared with the literature.

In this CMP, the supply curve is recalibrated based on the information provided by Hanssen et al. (2020). In particular, a lower supply price at the maximum availability is used, i.e., decreased from 10 US\$<sub>1975</sub>/GJ to about 6 US\$<sub>1975</sub>/GJ. As a result, the residual biomass supply curve shifts moderately towards the bottom left and is more consistent with the literature. It is worth noting that the supply curve for forestry residues (both primary and secondary) is tied to forestry products which are produced using managed forest land, not unmanaged forest land.

## 2.7. Other updates in assumptions driving biomass market expansion

GCAM traces the energy and emission flows and their corresponding monetary values. The flow chart for advanced bioenergy supply and demand is shown in **Fig. 3**. The primary bioenergy supply includes purpose-grown bioenergy crops, residues, and municipal solid waste (MSW). A

logit-based Armington framework is used for connecting future regional supply to regional demand.

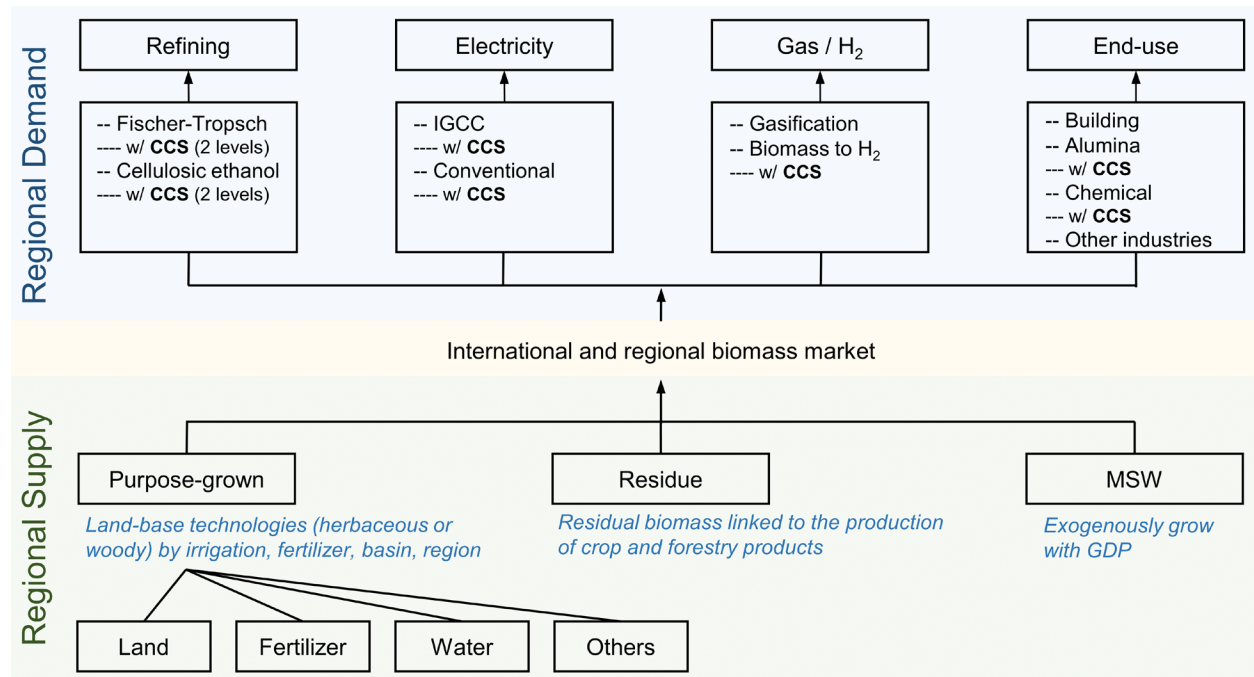


Fig. 3 Schematic of biomass flows in GCAM. IGCC stands for integrated gasification combined cycle. Note that w / CCS indicates the technology has the option of using carbon capture and sequestration (CCS) technologies under mitigation policies.

The following assumption changes were made in this CMP to enhance the representation of biomass market integration across time and regions:

- (1) A weaker global market integration trend is assumed for biomass. While GCAM initially assumed that the share-weights of domestic and imported biomass would fully converge by 2050, implying a global market, we have adjusted this to 50% (imported over domestic) to reflect a "home bias" in the market.
- (2) For the mature-year of dedicated energy crops, the values for pasture were used. In this CMP, 5-year and 8-year values are now used for herbaceous and woody biomass crops, respectively, in the latest version of GCAM.

More details of these technical changes can be found in gcamdata files summarized in Table 1.

## 2.8. Overview of key changes in gcamdata

Key data and code changes made in gcamdata are summarized in **Table 1**. In addition to key changes summarized in Sections 2.1-2.8, a few minor bugfixes are also included in this CMP, e.g., forestry trade parameters, chunk renaming, and intraregional trade removal.

Table 1 key data and code changes made in gcamdata

Data file or R chunk	Changes made
region_minicam.cpp	Update social discount rate. (DEFAULT_SOCIAL_DISCOUNT_RATE = 0.03)
constants.R zaglu_L2252.land_input_5_irr_mgmt.R	biomassGrass_mature_age = 5 and biomassTree_mature_age = 8
module-helpers.R	Adding the option of “Min_Soil_C_at_Cropland = TRUE” to the function of add_carbon_info().
zaglu_L2242.land_input_4_irr_mgmt.R A_bio_ghost_share.csv A_biomassSupplyShare_R.csv	Capability to easily differentiate assumptions in purpose-grown energy cropland introduction (ghost-share) by region. Note that the original assumptions were not changed.
A_bio_subsector.csv	Update future integration assumptions in biomass trade.
A_demand_nesting_subsector.csv A_demand_subsector.csv A_demand_supplysector.csv A_demand_technology.csv	Update logit exponent to represent food substitution. FiberCrop is moved to the Oil nest since over 99% of the FiberCrop for food consumption is cottonseed oil.
zaglu_L221.land_input_1.R	Adding the default option of “UsingGCAMCroplandRentalProfit = TRUE” and related code
zaglu_L222.land_input_2.R zaglu_L2231.land_input_3_irr.R	Update the add_carbon_info().
zenergy_L222.en_transformation.R A22.SubsectorInterp_en_R.csv A22.SubsectorShrwtFlt_en_R.csv	Capability to easily differentiate biomass share-weight assumption in transformation sectors by region. Note that the original assumptions were not changed.
A_LandNode_logit.csv A_LandNode_logit_irr.csv	Update land logit exponent.
A_resbio_curves.csv	Update the residual biomass supply curve.
A_agRegionalSector.csv A_agTradedSector.csv	Update roundwood trade parameters.
zaglu_L133.ag_Costs_C_2005.R zaglu_L164.ag_Costs_C_2005_irr.R	Renamed as they were miscategorized to other modules.
zaglu_L120.LC_GIS_R_LTgis_Yh_GL U.R	Remove “aglu/LDS/L123.LC_bm2_R_MgdFor_Yh_GLU_beforeadjust.csv” and related code.
zaglu_L100.FAO_SUA_PrimaryEquivalent.R	Remove intraregional Ag. trade. Unit was wrong previously so the removal was divided by 1000.

### 3. Shared policy assumption (SPA) GCAM validation runs

In accordance with the GCAM CMP convention, we present GCAM projection results, comparing the Updated (Para.) branch with the Master branch (CMP-392) for reference and RCP 2.6 scenarios across shared socioeconomic pathways (GCAM core & SSP1-5 assumptions; excluding SSP3-RCP2p6). We provide key global results in the figures below, with detailed regional and sectoral results available in Supplementary Figures. The key impact of the updates and insights are summarized as follows:

Land use change emissions are significantly lower for most scenarios in both ref. and 2p6 scenarios (Figs 4 & 5), mainly driven by the corresponding forest land use change (Figs 8 & 9).

- For ref. scenarios, it was because of the less pronounced deforestation. In addition, other natural land and nonenergy cropland in ref. became relatively smaller with the updates in ref. scenarios.
- In 2p6 scenarios, afforestation/reforestation becomes much stronger with the updates in land mitigation policy, as the land carbon policies become more effective with the updates. And nonenergy cropland reduction becomes smaller while more other natural land (grass & shrubland) is converted.
- In all ref. scenarios, the fossil fuels and industry (FFI) carbon dioxide emissions increased, though the total carbon emission did not increase as much since FFI emissions are offset by the lower emissions from land use change. The FFI emission increase were partly driven by the lower bioenergy consumption (Figs 10 – 12). The directions of emission changes are mixed in 2p6 scenarios (Fig. 4).

Overall, climate variables, forcing, temperature change, and concentration, were not significantly affected (Figs. 6 & 7). However, there was a relatively larger change in net terrestrial carbon uptake (Fig. 6). It appears that lower LULUCF emissions, e.g., driven by higher afforestation, could create a synergy with natural land carbon sinks, especially in scenarios with additional afforestation due to the updates, e.g., in all scenarios except for RCP2p6-core and RCP2p6-SSP2.

- Note that SSP2 and core have none or lower LULUCF emission decrease due to the updates in the CMP, compared to other scenarios; even though there is a global net increase in forest, other natural land decreases relatively more.
- The net terrestrial carbon uptake moderately decreased in the SSP2 and core scenarios under 2p6, while the additional uptake was significant in other SSPs, leading to additional allowance in FFI emissions (Fig. 4) and lower carbon prices in those scenarios (Fig. 7). This explains the significantly lower carbon prices (Fig. 7) under RCP2p6 for SSP1, 4 & 5, but relatively higher carbon prices in core and SSP2, due to the updates.

In all scenarios, more other arable land (unused cropland) is converted for other uses in mitigation runs, e.g., about 100 Mha by 2100 in core by 2100 (Fig. 9). This was mainly due to the adjustment of lower land logit exponent between cropland and other lands so that relatively more crop expansion into "other arable land", i.e., within the cropland nest, is seen. The updates of shadow rental profit for other arable land may also played a role.

Biomass supply decreased in the ref scenarios while the change is more region- and scenario-dependent in 2p6 scenarios (relatively small globally) (Figs 10 & 11).

- Residual biomass supply is driven by crop supply, and the share of the supply reaches the peak earlier, given the updated residual biomass supply curve (Fig. 11). However, the relatively higher crop production also encourages an increased residue biomass supply in 2p6.
- Impacts on biomass demand and BECCS are also mixed with high regional differences, and there could be transitions of biomass use between non/low-BECCS sector and (high-)BECCS sectors (Fig. 12).

When allowing more flexible food substitution, moderate substitution was seen within both staples and nonstaple nests (Fig. 13 & Fig. S1). Fish (and other meats) consumption increased in mitigation scenarios. Agricultural prices decreased significantly (Fig. 14), and total calorie consumption increased. African regions experienced the largest changes. Previously, the price of a few crops could increase by over 10 times by 2100 in mitigation scenarios in African regions, and the price increases were significantly lower after the updates (Fig. S2).

The impacts from the updates on the total agricultural fertilizer consumption and water withdrawal are mostly smaller (Figs. 15 & 16). Changes in nonCO<sub>2</sub> GHG emissions were also moderate (Fig. 17).

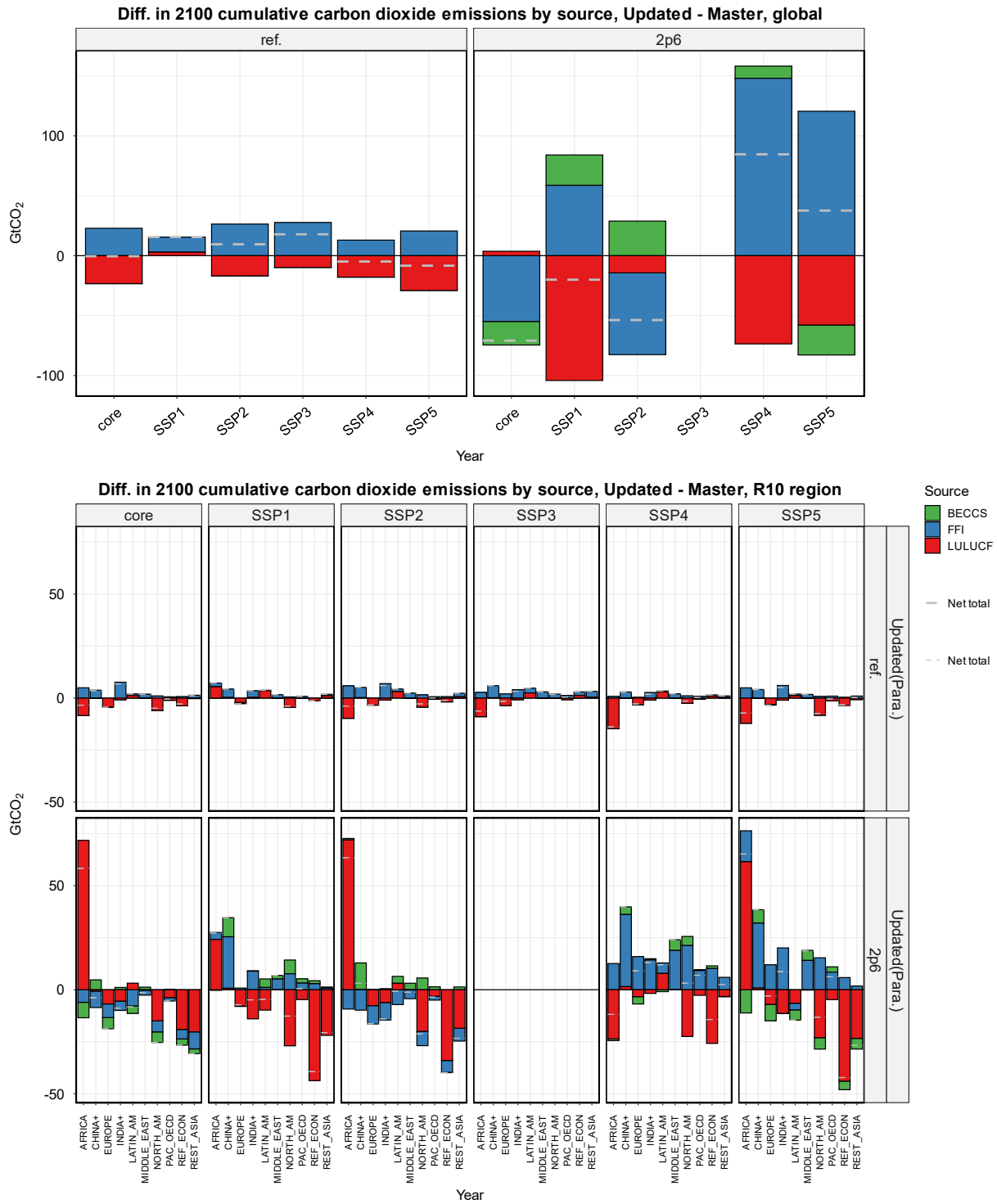


Fig. 4 Global and regional changes in cumulative carbon dioxide emissions in 2020 - 2100. LULUCF stands for Land Use, Land-Use Change and Forestry.

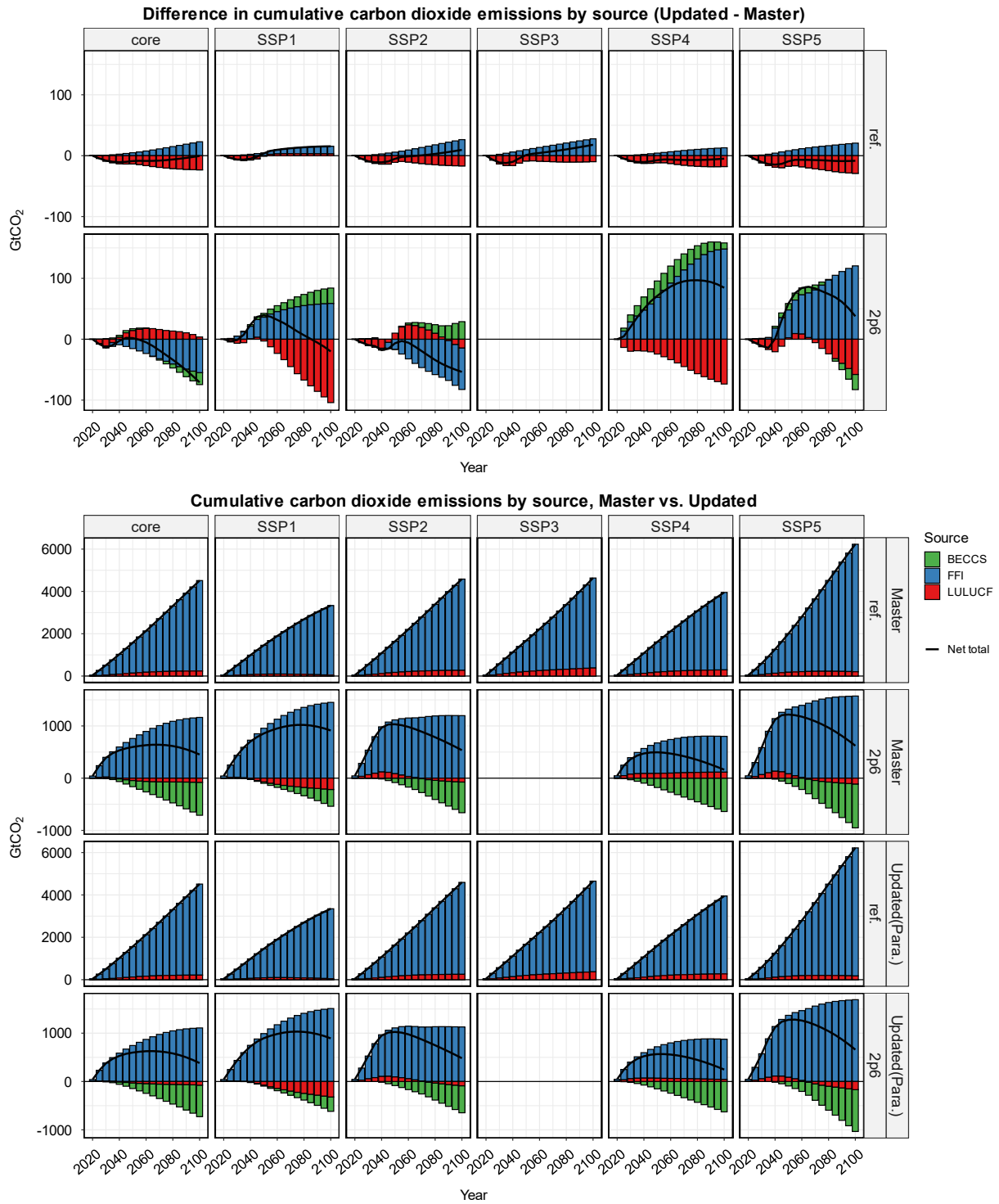


Fig. 5 Cumulative carbon dioxide emissions (starting 2020).

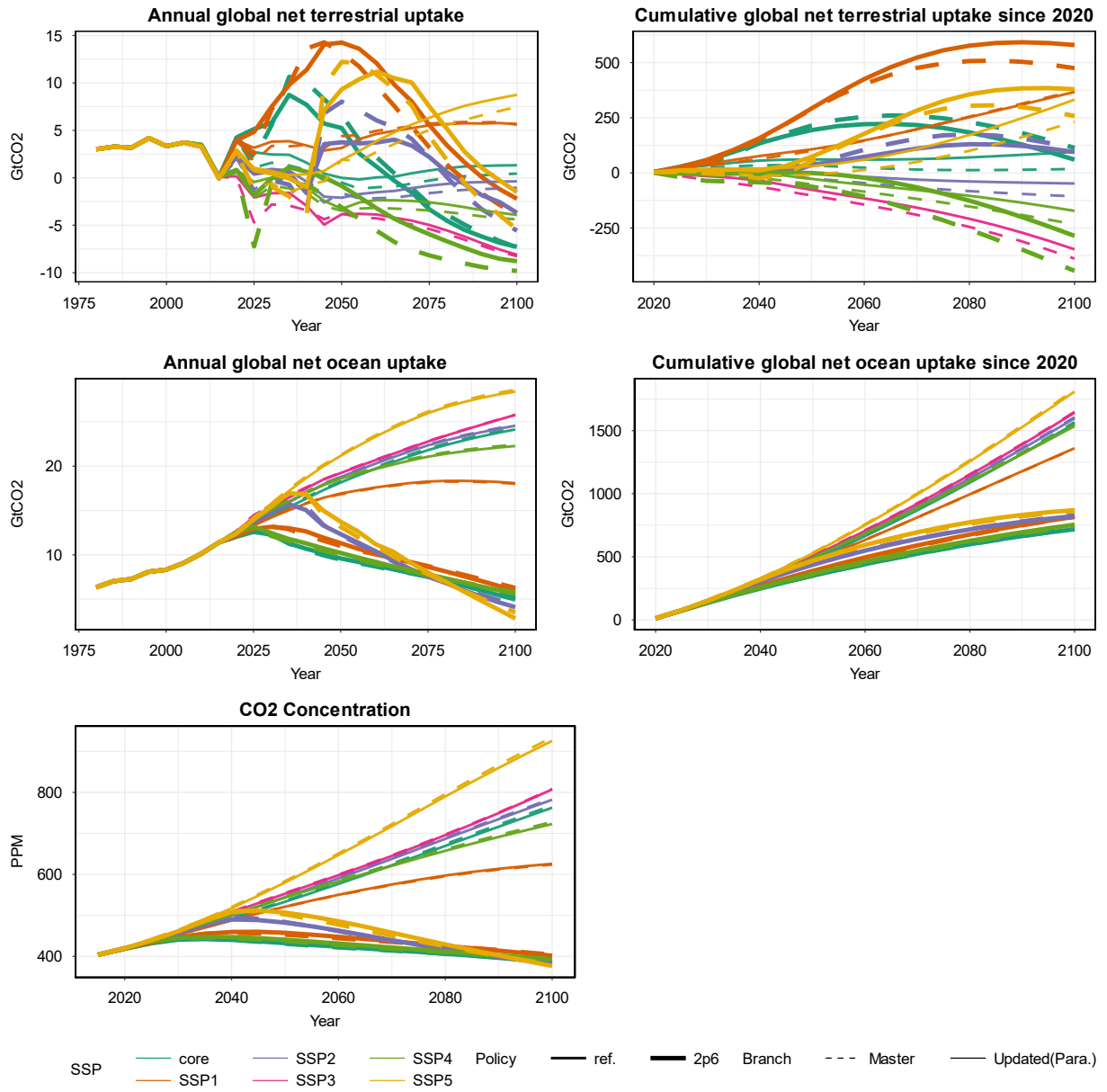


Fig. 6 Global net carbon uptakes in terrestrial and ocean systems and atmosphere carbon concentration.

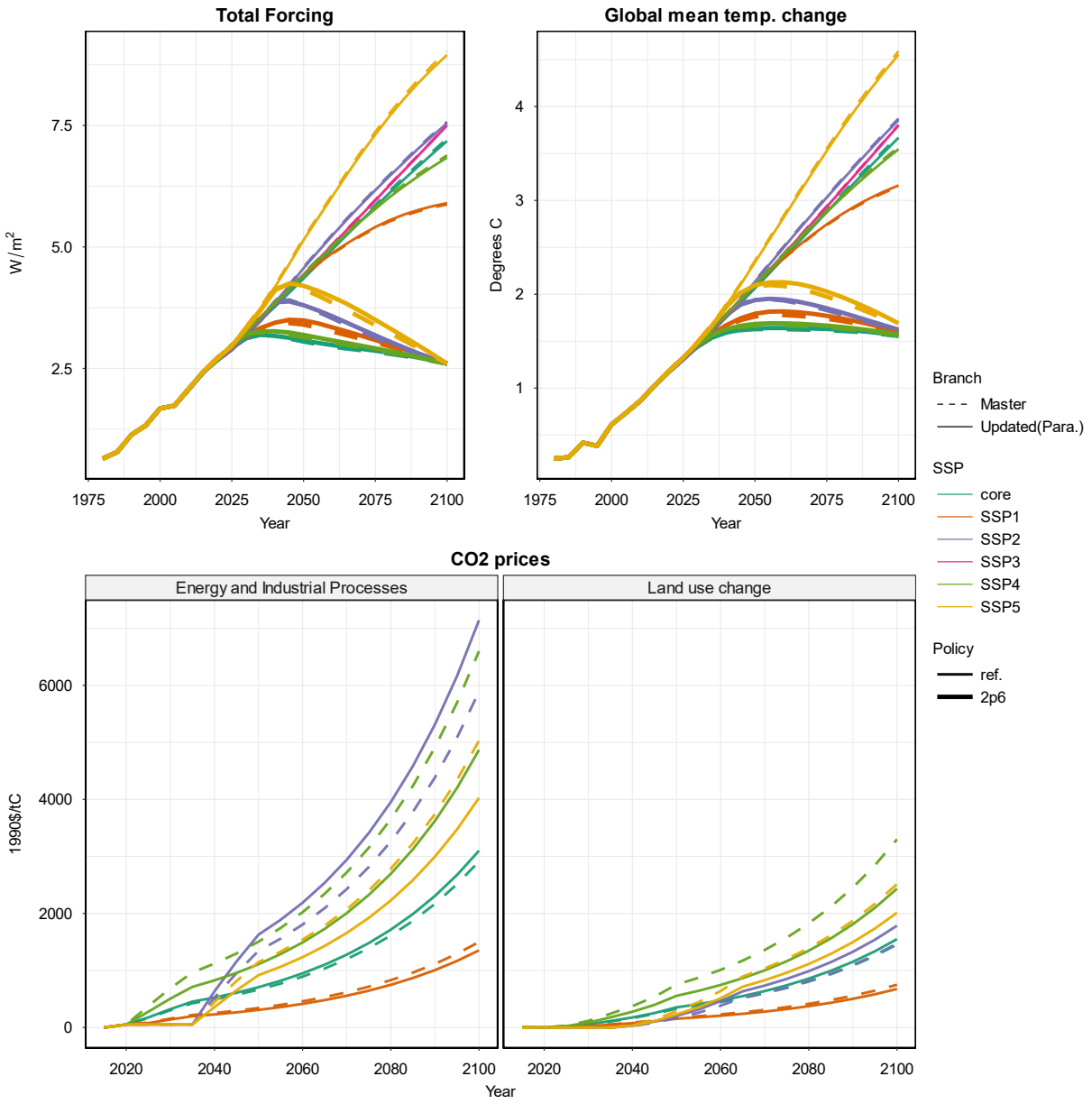


Fig. 7 Forcing, mean temperature change, and carbon prices.

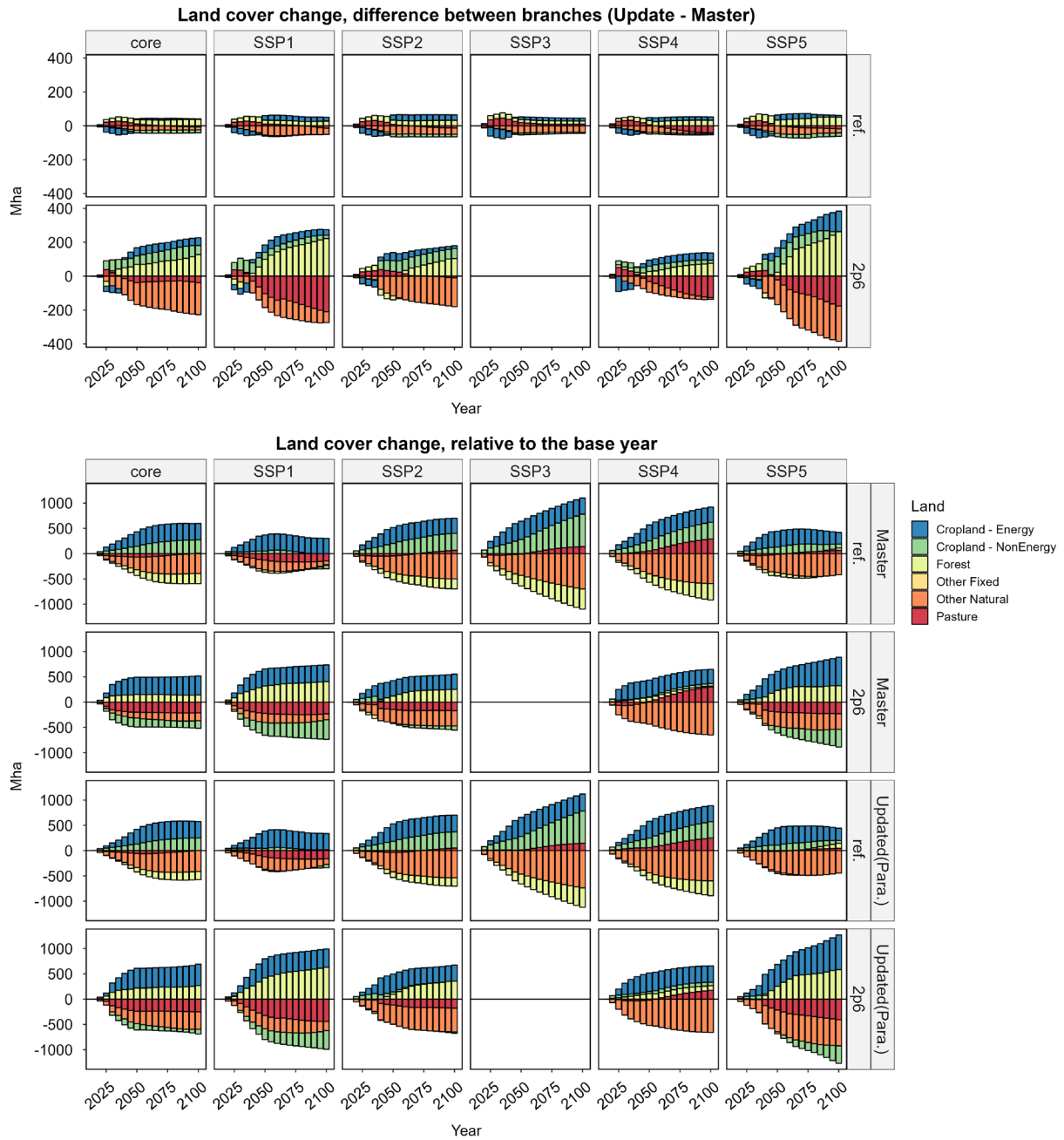


Fig. 8 Global land use change.

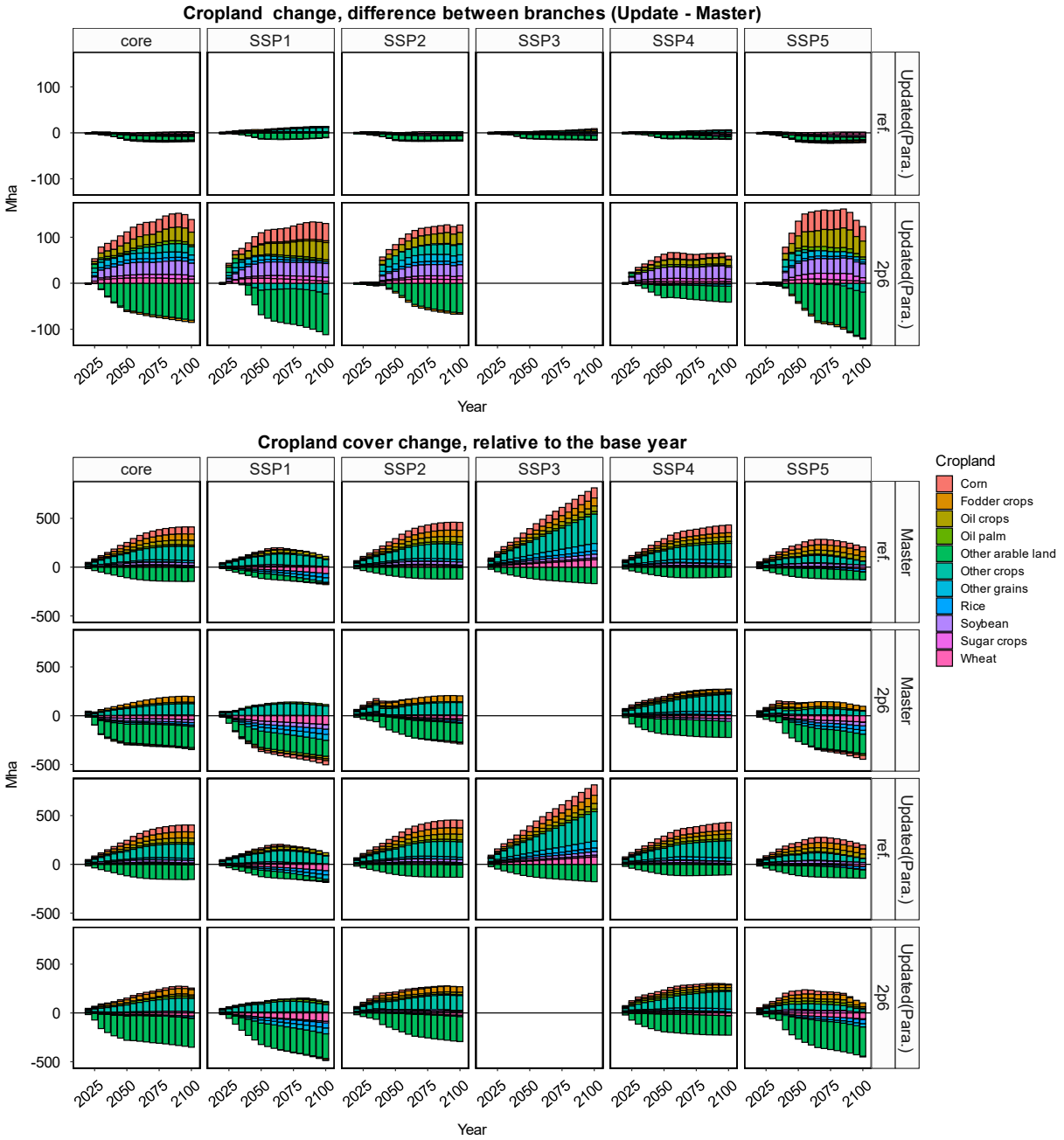


Fig. 9 Global cropland change.

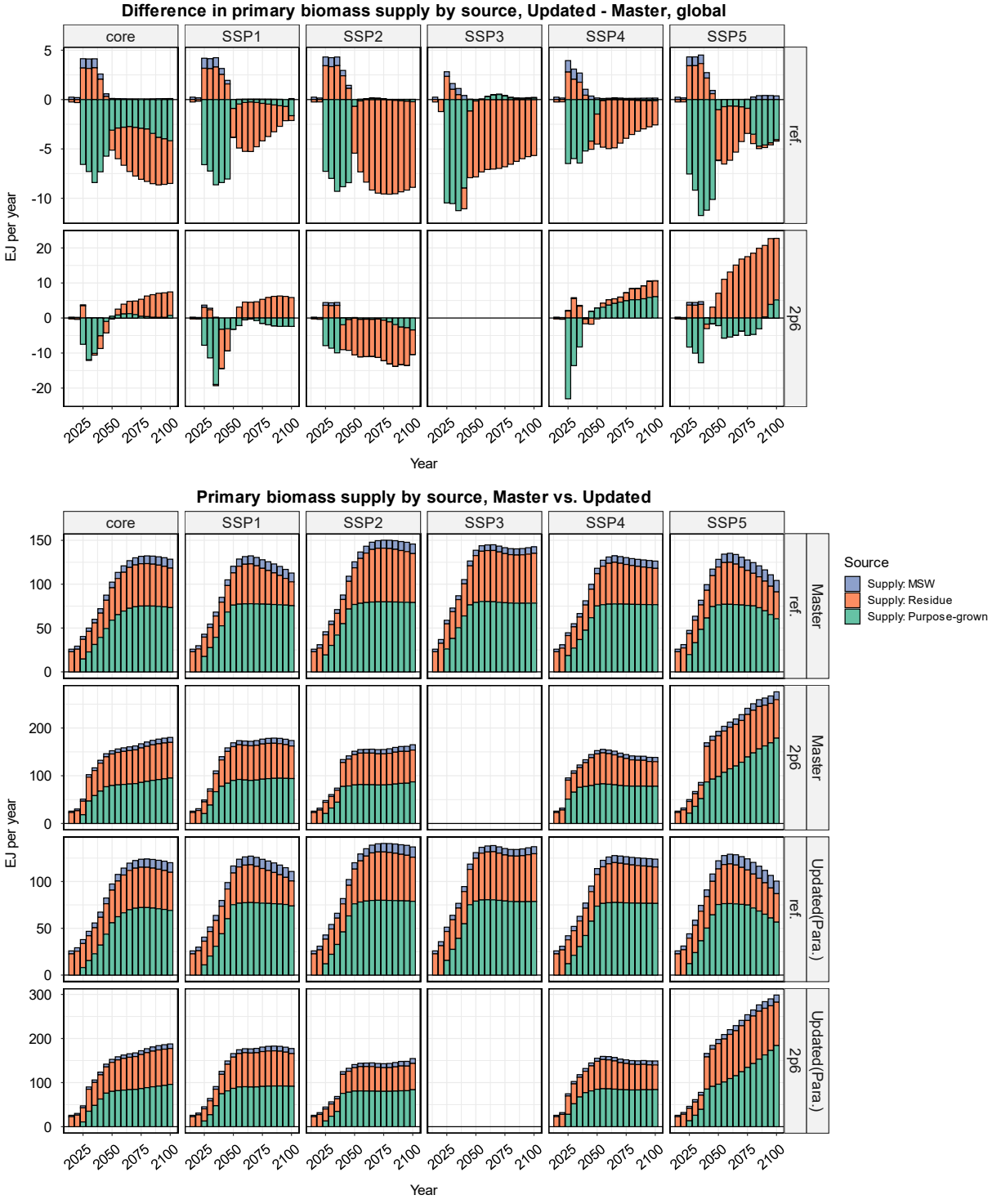


Fig. 10 Global primary biomass supply by source.

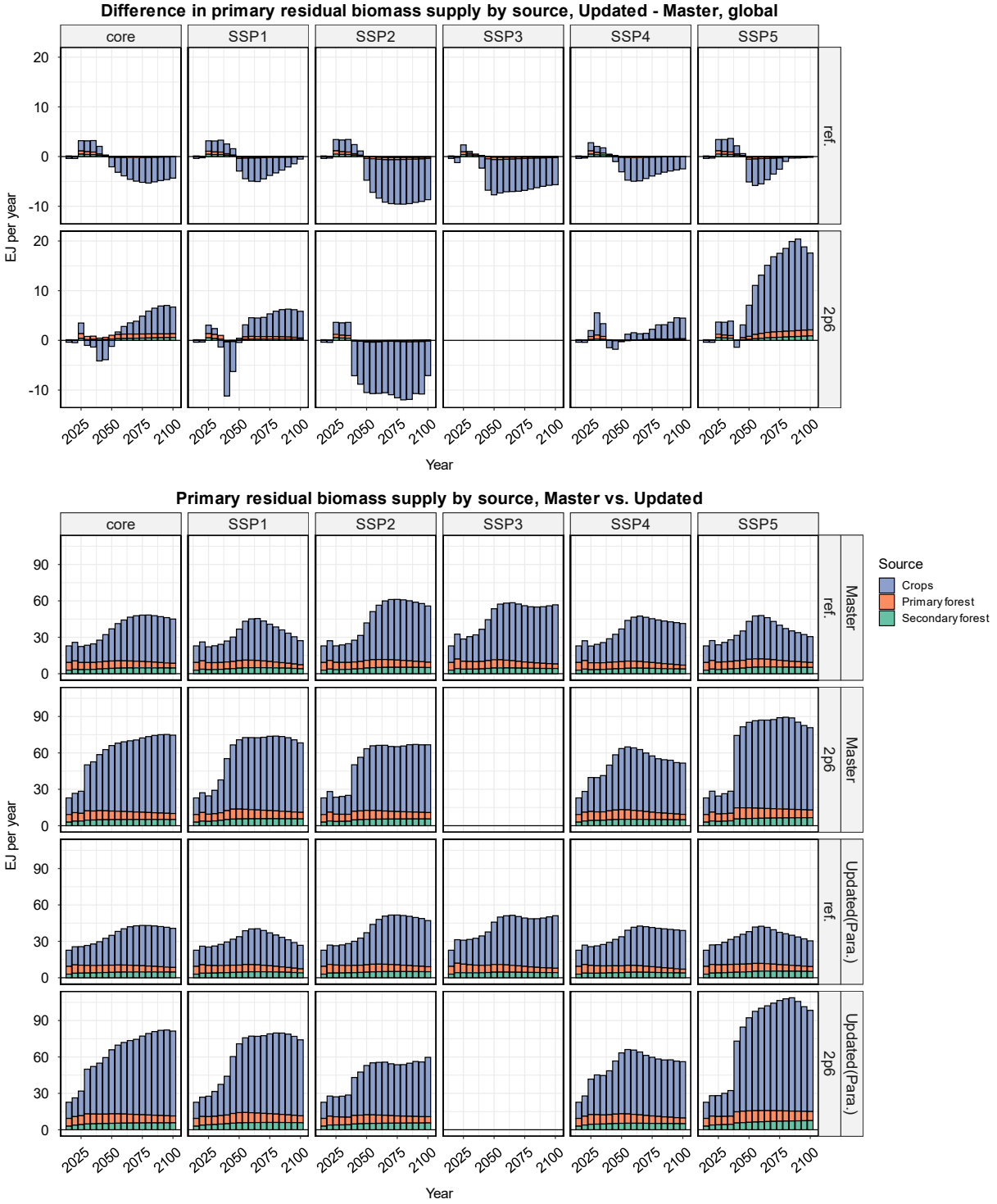


Fig. 11 Global residual biomass supply by source.

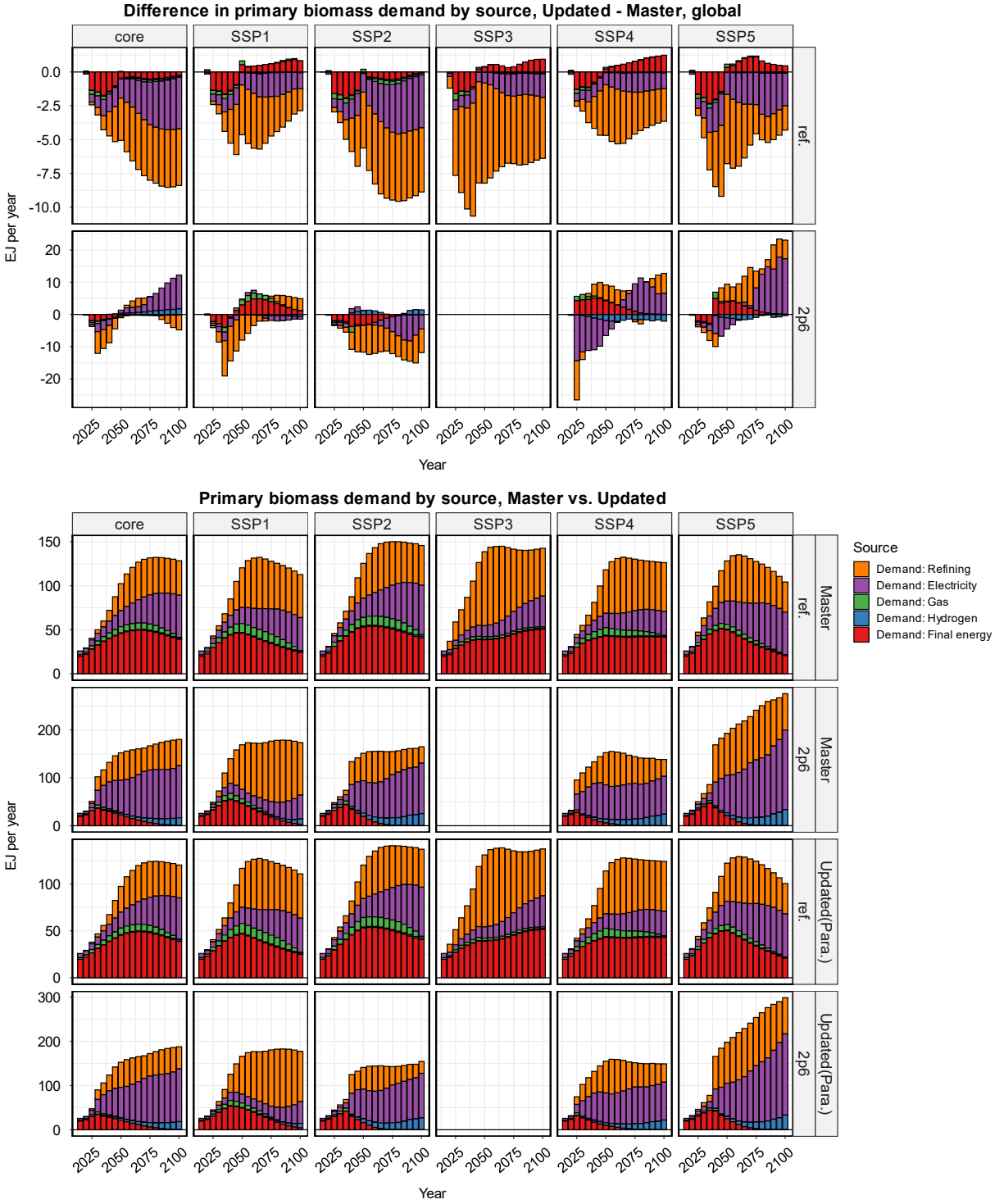


Fig. 12 Global biomass demand by source.

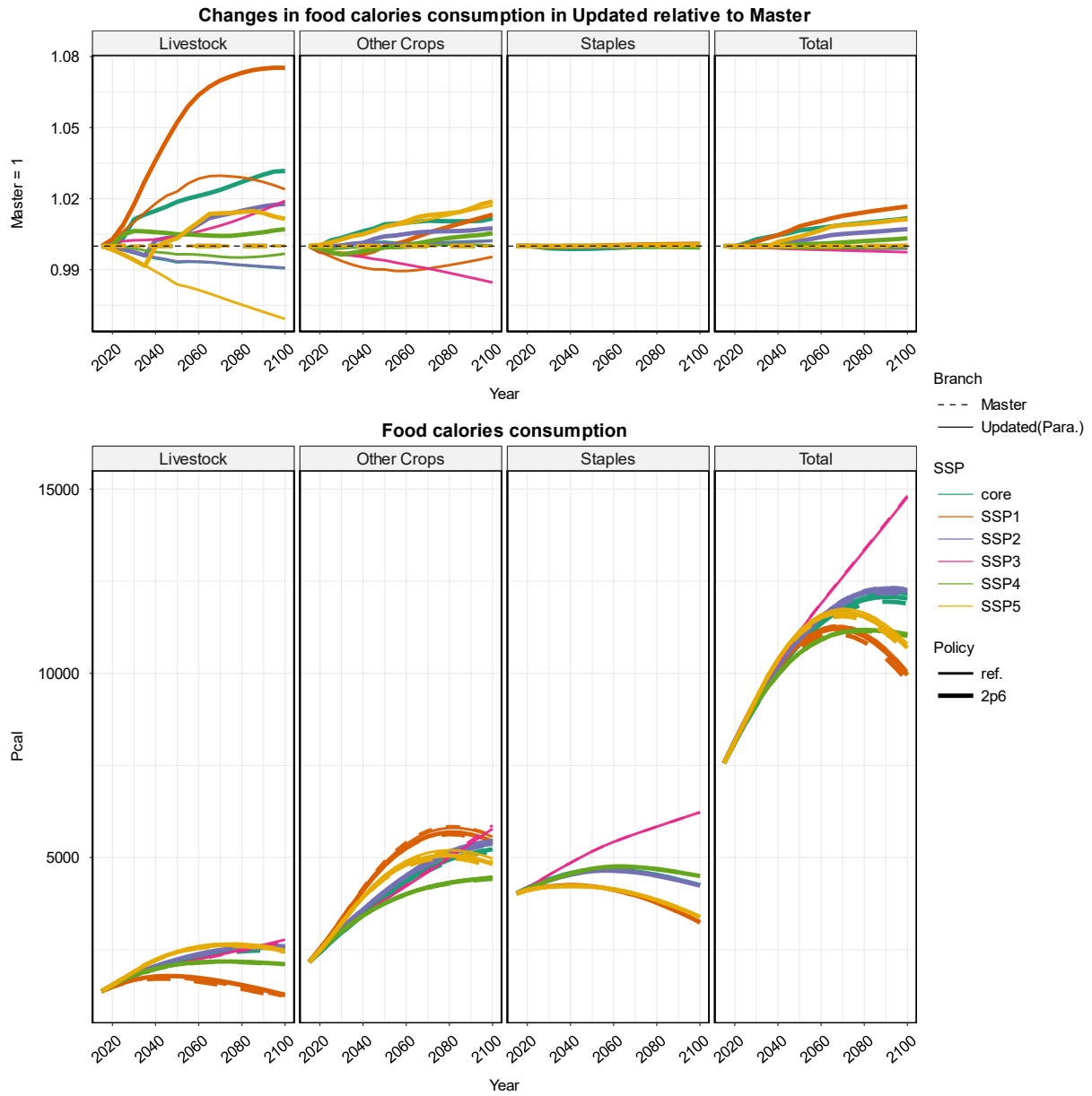


Fig. 13 Global food calorie consumption supply by source.

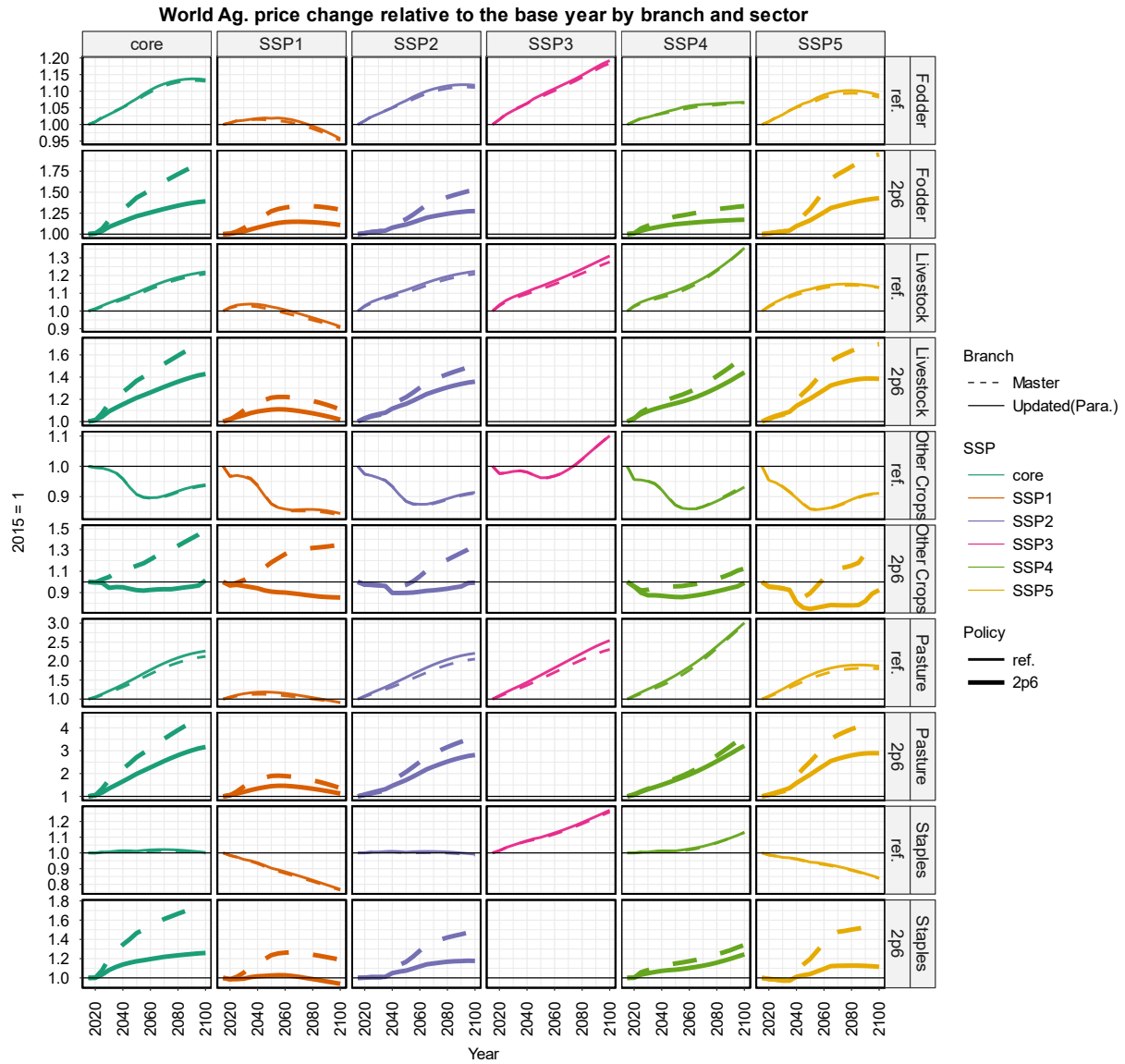


Fig. 14 Global agricultural prices by sector.

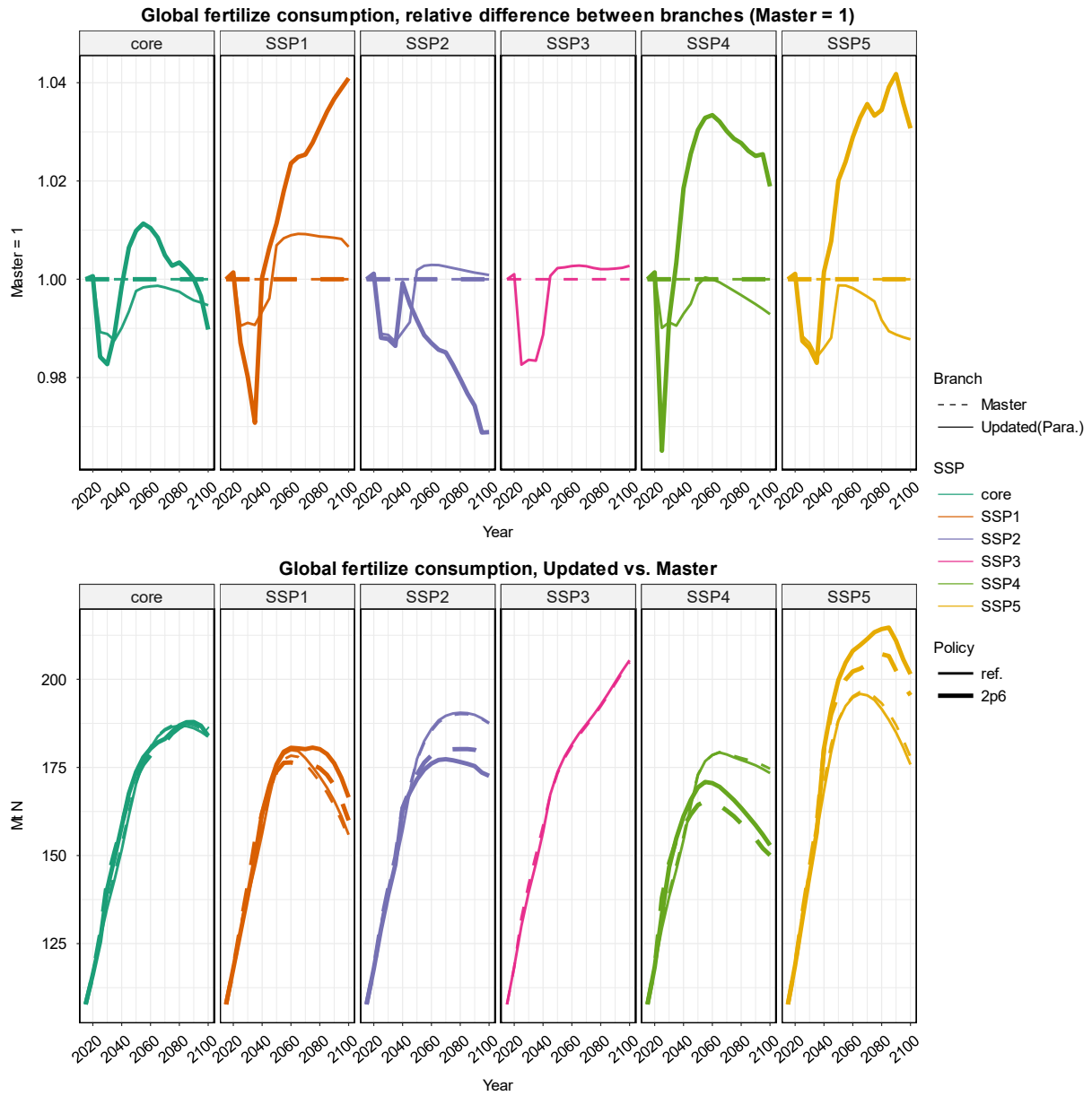


Fig. 15 Global fertilizer consumption changes.

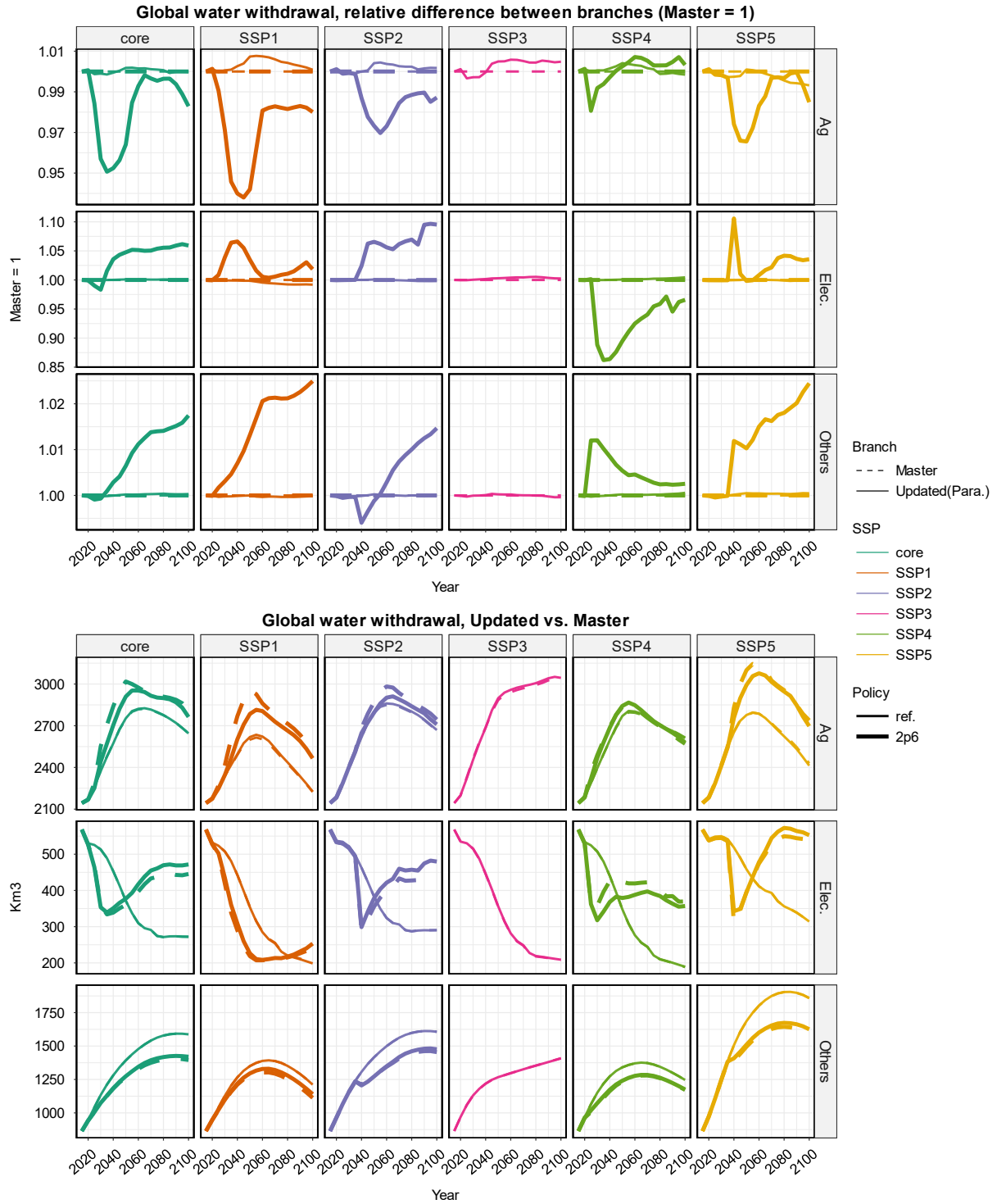


Fig. 16 Global water withdrawal changes by sector.

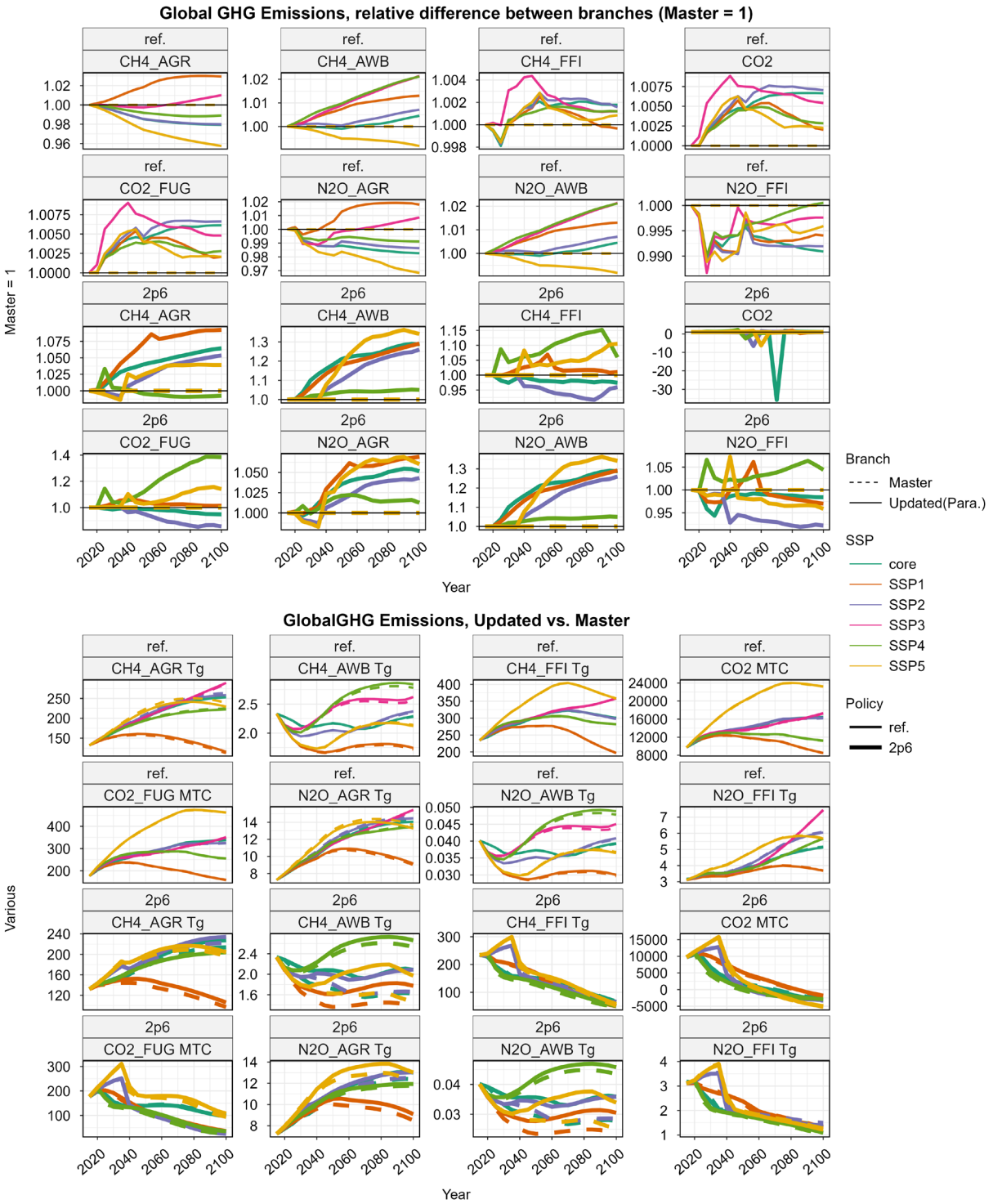


Fig. 17 Global GHG (CO<sub>2</sub>, CH<sub>4</sub>, and N<sub>2</sub>O) emissions.

#### 4. Summary and future work

This CMP documents the changes in GCAM parameters and assumptions related to (1) land allocation (e.g., primarily a lower logit exponent to enhance behavior), (2) the implementation of land carbon pricing policy, (3) food demand (allowing for price-induced dietary changes), and (4) the supply (mainly residues) and trade of primary biomass. These changes were included in Zhao et al. (2024b) for studying land-based mitigation measures, i.e., universal land carbon tax, afforestation/reforestation, and bioenergy in combination with carbon capture and sequestration). With these changes, agro-economic projections related to land allocation, dietary changes, agricultural and food prices, land use change emissions, and land-based mitigation policy implications are improved. Projections generated by the model are notably influenced by the underlying assumptions regarding parameters. Regularly reviewing and updating these assumptions with the latest information is crucial for enhancing the robustness of the modeling and projection outcomes.

A few areas for improvement in future work:

- 1) Regional parameters of biomass supply can be explored in future work. In GCAM (v7), purpose-grown energy cropland was introduced by gradually increasing the land logit share-weight since 2025. On the demand side, the share-weights of biomass liquids in the refining sector were also assumed to converge to 1 over time (e.g., by 2030). The model currently does not differentiate changes in preference (share-weights) drivers by region, and the changes over time were fairly strong. Zhao et al. (2024b) tested differentiating both (1) the rate of introduction (biomass land share-weights) of biomass cropland and (2) the biomass liquid preference change (refining share-weights) by region. Particularly, in regions without current efforts to support bioenergy, including first-generation bioenergy, such as African regions, a relatively lower expansion rate in the corresponding share-weights was assumed.
- 2) Technological changes in the livestock sectors: Currently, GCAM does not allow for future changes in livestock intensification driven by exogenous technological progress. Related assumptions were included in Zhao et al. (2024b). However, they are not incorporated into this CMP since additional assumptions are needed to differentiate the scenario across SSPs.
- 3) Data processing issues in the downscaling process of crop yield in gcamdata: We have recently identified issues leading to potential extreme values in crop yield in a few regions/basins. While these regions are small, they tend to be more responsive in policy runs. A bugfix branch has been created, but it was not included in this CMP to avoid complications in reviewing and difficulties in validation runs.
- 4) Inclusion of both first- and second-generation bioenergy feedstock in the negative emission budget limit constraint: Currently, this is done to represent macroeconomic constraints on supporting negative emission technologies. However, GCAM and most models do not link

all intermediate/indirect emissions to the bioenergy production life-cycle. These areas could be explored further.

- 5) Residual biomass availability. In Zhao et al. (2024b), a 10% requirement for other uses (e.g., animal bedding) (Searle and Malins, 2015) and 5% – 20% dry matter loss (Cafferty et al., 2014; Smith et al., 2020) were also added when determining the maximum residual biomass energy available for crops. These assumptions can be examined and explored further.

# Supplementary Information

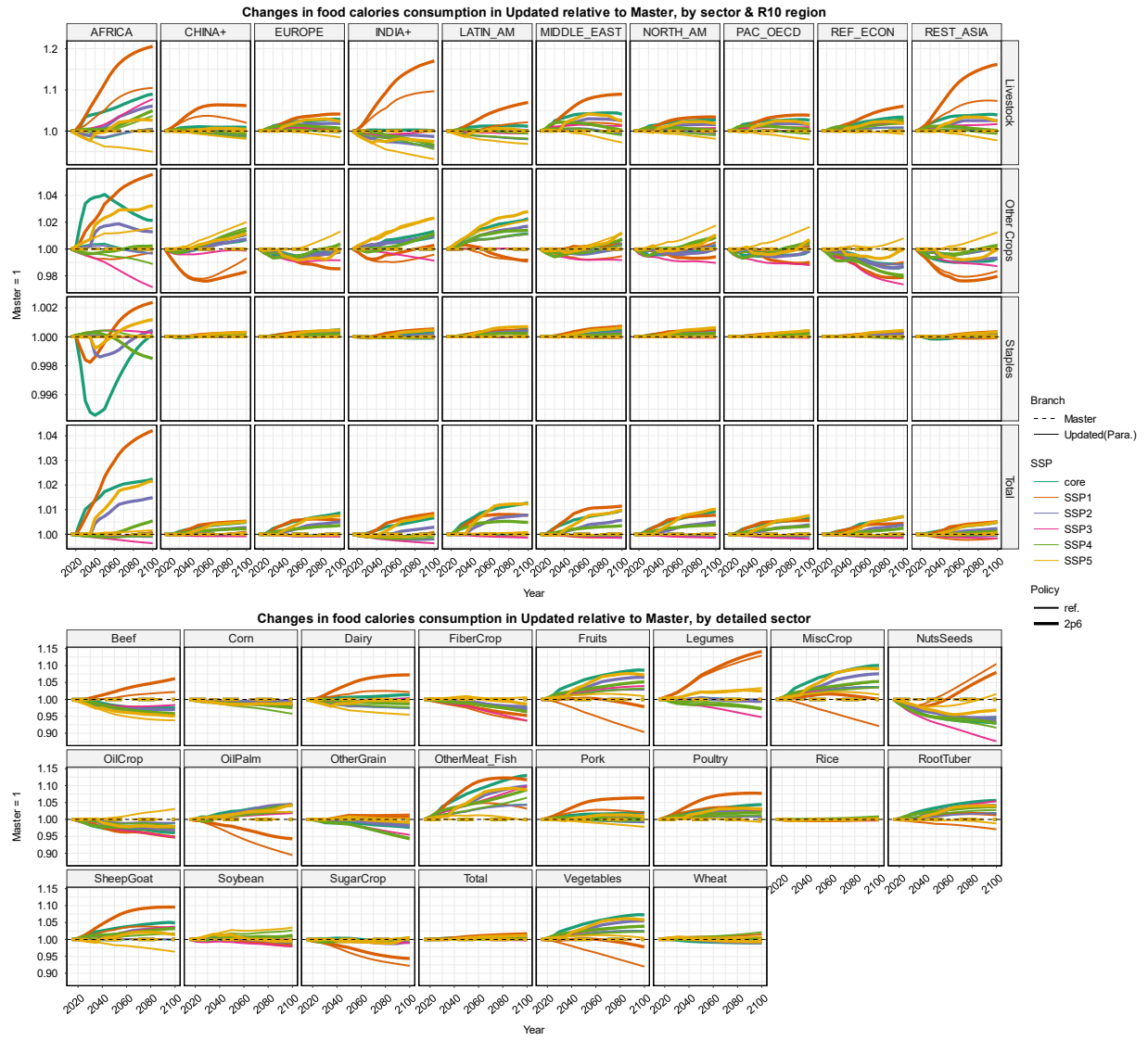


Fig. S1 Impacts on food calorie consumption by region and sector.

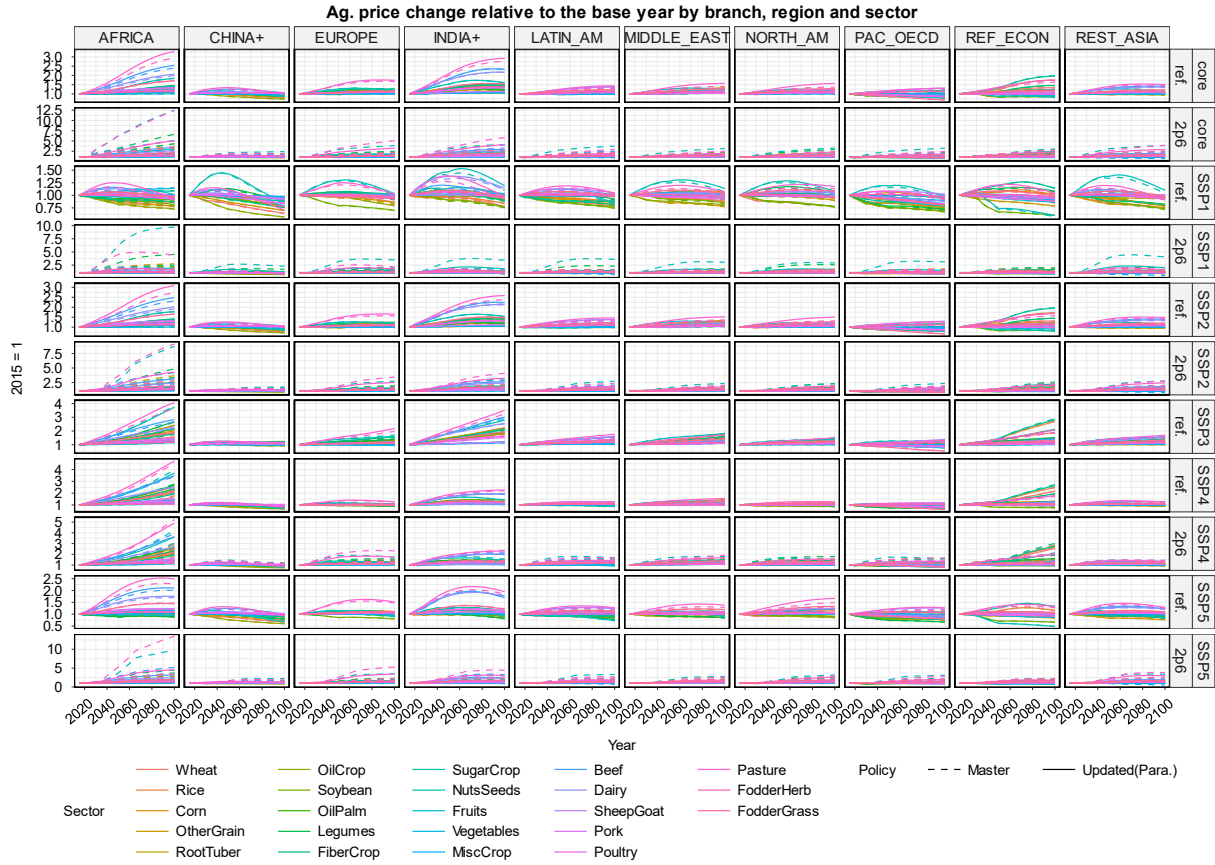


Fig. S2 Impacts on agricultural prices by region and sector.

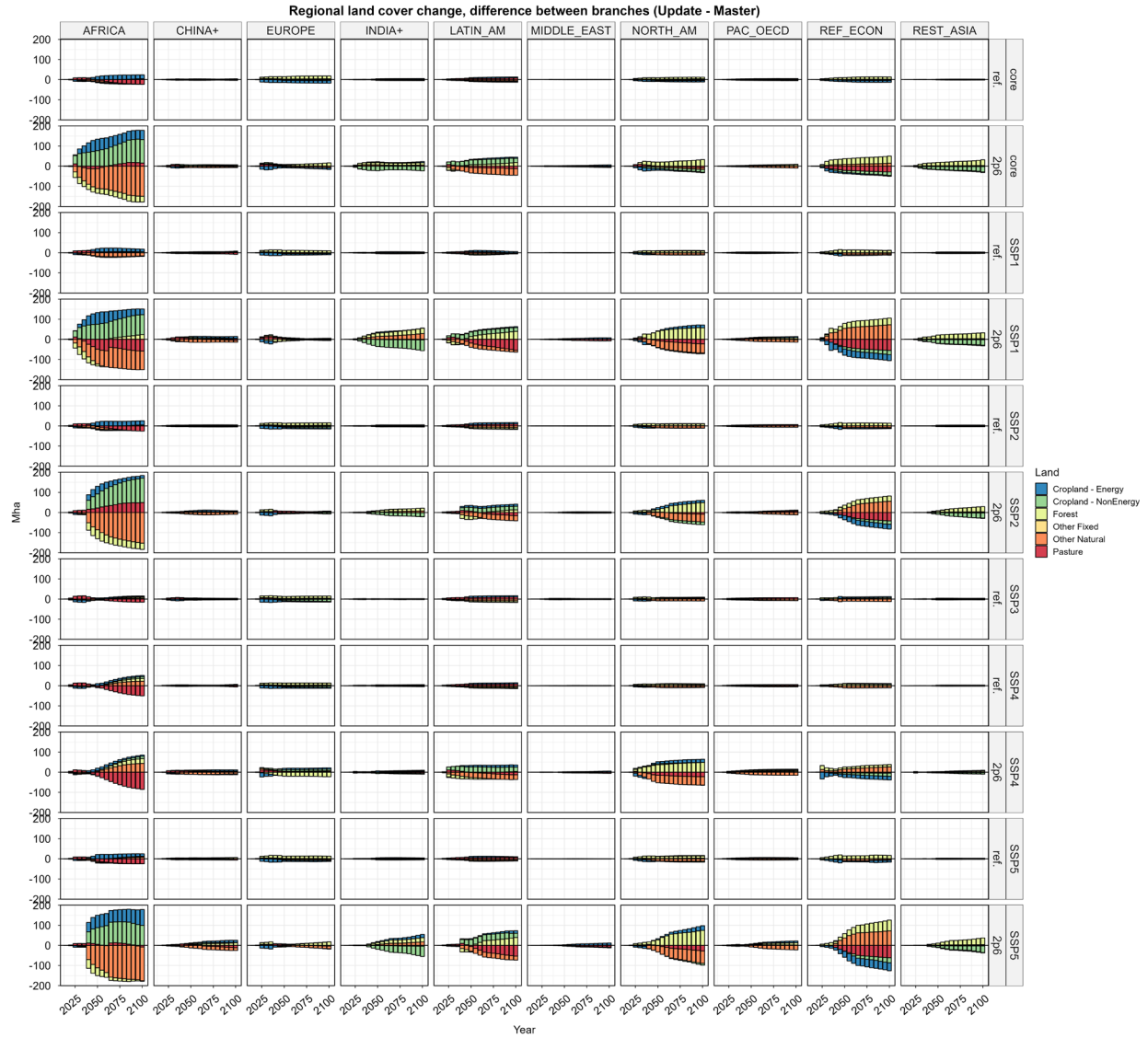


Fig. S3 Impacts on regional land use.

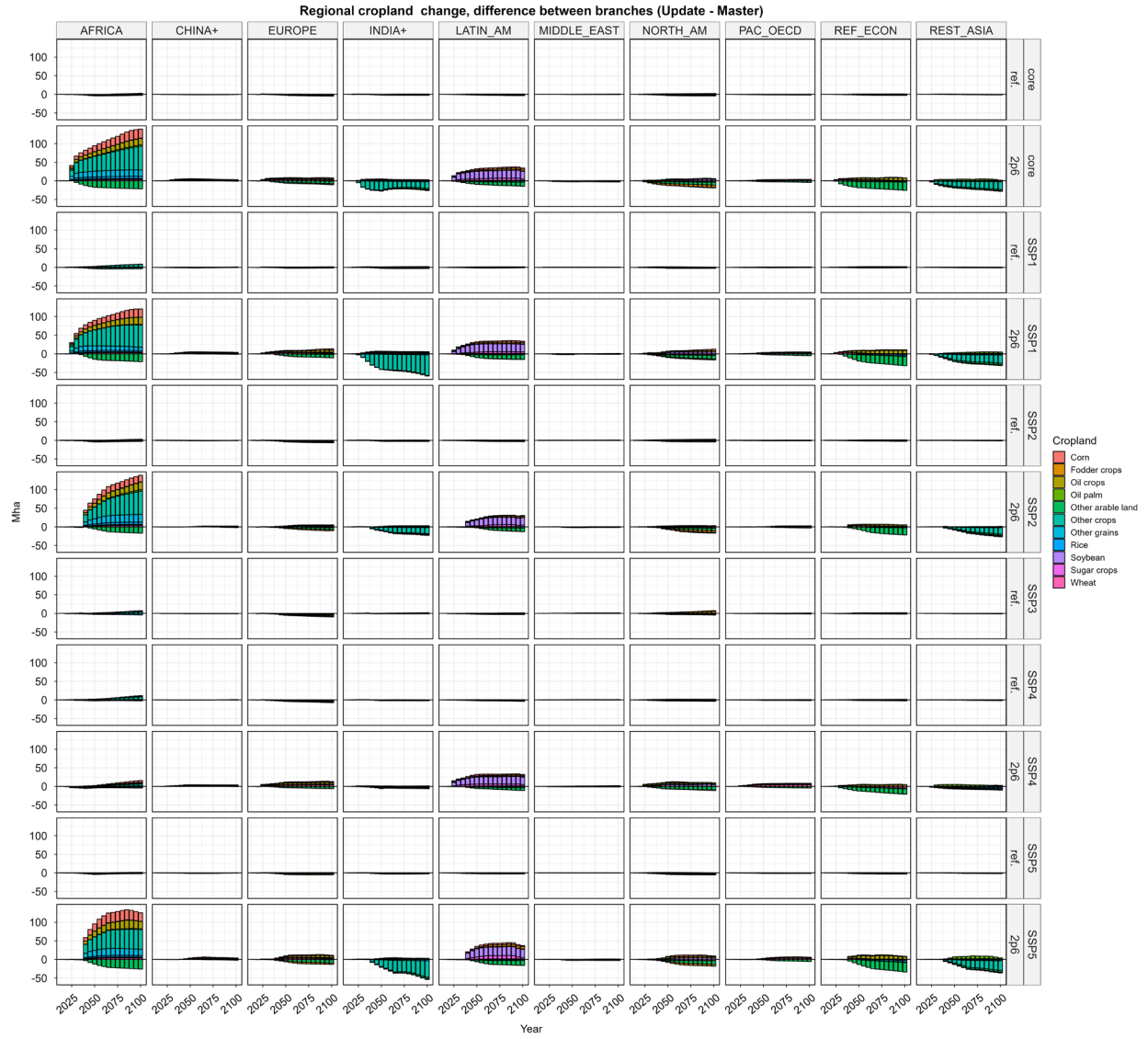


Fig. S4 Impacts on regional cropland.

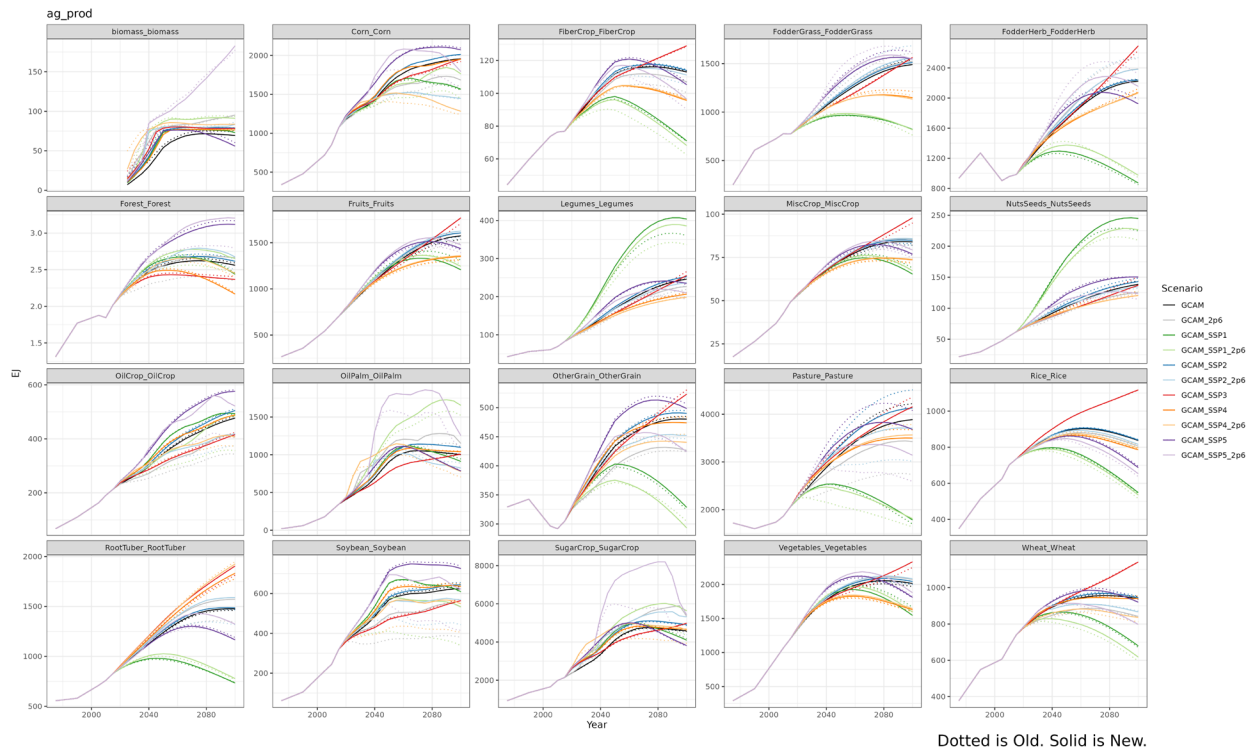


Fig. S5 Impacts on agricultural production. There is overall more elastic cropland supply due to the updates so that the impact (decrease) due to mitigation policy on cropland will be smaller (First generation bioenergy is also affected less by mitigation polices).

## References

- Ahmed, S.A., Hertel, T., Lubowski, R., 2008. Calibration of a Land Cover Supply Function Using Transition Probabilities [WWW Document]. GTAP Research Memorandum No. 14, GTAP Research Memorandum No. 14. URL [http://www.gtap.agecon.purdue.edu/resources/res\\_display.asp?RecordID=2947](http://www.gtap.agecon.purdue.edu/resources/res_display.asp?RecordID=2947)
- Cafferty, K.G., Muth, D.J., Jacobson, J.J., Bryden, K.M., 2014. Model Based Biomass System Design of Feedstock Supply Systems for Bioenergy Production. Presented at the ASME 2013 International Design Engineering Technical Conferences and Computers and Information in Engineering Conference, American Society of Mechanical Engineers Digital Collection. <https://doi.org/10.1115/DETC2013-13559>
- Calvin, K., Patel, P., Clarke, L., Asrar, G., Bond-Lamberty, B., Cui, R.Y., Di Vittorio, A., Dorheim, K., Edmonds, J., Hartin, C., Hejazi, M., Horowitz, R., Iyer, G., Kyle, P., Kim, S., Link, R., McJeon, H., Smith, S.J., Snyder, A., Waldhoff, S., Wise, M., 2019. GCAM v5.1: representing the linkages between energy, water, land, climate, and economic systems. *Geoscientific Model Development* 12, 677–698. <https://doi.org/10.5194/gmd-12-677-2019>
- Di Vittorio, A.V., Narayan, K.B., Patel, P., Calvin, K., Vernon, C.R., 2023. Doubling protected land area may be inefficient at preserving the extent of undeveloped land and could cause substantial regional shifts in land use. *GCB Bioenergy* 15, 185–207. <https://doi.org/10.1111/gcbb.13016>
- Di Vittorio, A.V., Vernon, C.R., Shu, S., 2020. Moirai Version 3: A Data Processing System to Generate Recent Historical Land Inputs for Global Modeling Applications at Various Scales 8, 1. <https://doi.org/10.5334/jors.266>
- Edmonds, J.A., Link, R., Waldhoff, S.T., Cui, R., 2017. A global food demand model for the assessment of complex human-earth systems. *Clim. Change Econ.* 08, 1750012. <https://doi.org/10.1142/S2010007817500129>
- Ferreira Filho, J.B. de S., Ribera, L., Horrigan, M., 2015. Deforestation Control and Agricultural Supply in Brazil. *American Journal of Agricultural Economics* 97, 589–601. <https://doi.org/10.1093/ajae/aav004>
- Fujimori, S., Hasegawa, T., Masui, T., Takahashi, K., 2014. Land use representation in a global CGE model for long-term simulation: CET vs. logit functions. *Food Sec.* 6, 685–699. <https://doi.org/10.1007/s12571-014-0375-z>
- Gregg, J.S., Smith, S.J., 2010. Global and regional potential for bioenergy from agricultural and forestry residue biomass. *Mitig Adapt Strateg Glob Change* 15, 241–262. <https://doi.org/10.1007/s11027-010-9215-4>
- Hanssen, S.V., Daioglou, V., Steinmann, Z.J.N., Frank, S., Popp, A., Brunelle, T., Lauri, P., Hasegawa, T., Huijbregts, M.A.J., Van Vuuren, D.P., 2020. Biomass residues as twenty-first century bioenergy feedstock—a comparison of eight integrated assessment models. *Climatic Change* 163, 1569–1586. <https://doi.org/10.1007/s10584-019-02539-x>
- Hashida, Y., Lewis, D.J., 2019. The Intersection between Climate Adaptation, Mitigation, and Natural Resources: An Empirical Analysis of Forest Management. *Journal of the Association of Environmental and Resource Economists* 6, 893–926. <https://doi.org/10.1086/704517>
- IUCN, 2018. World database on protected areas [WWW Document]. URL <https://www.protectedplanet.net> (accessed 5.2.23).

- Li, C., Wu, J., 2022. Land use transformation and eco-environmental effects based on production-living-ecological spatial synergy: evidence from Shaanxi Province, China. *Environ Sci Pollut Res*. <https://doi.org/10.1007/s11356-022-18777-z>
- Lintunen, J., Laturi, J., Uusivuori, J., 2016. How should a forest carbon rent policy be implemented? *Forest Policy and Economics* 69, 31–39. <https://doi.org/10.1016/j.forpol.2016.04.005>
- Narayan, K., Vernon, C., Vittorio, A.D., EvanMargiotta, 2022. JGCRI/moirai: Moirai v3.1.1. <https://doi.org/10.5281/zenodo.6632745>
- Ramankutty, N., Hertel, T., Lee, H.-L., 2005. Global Land Use and Land Cover Data for Integrated Assessment Modeling [WWW Document]. GTAP, GTAP. URL [http://www.gtap.agecon.purdue.edu/resources/res\\_display.asp?RecordID=1635](http://www.gtap.agecon.purdue.edu/resources/res_display.asp?RecordID=1635)
- Searle, S., Malins, C., 2015. A reassessment of global bioenergy potential in 2050. *GCB Bioenergy* 7, 328–336. <https://doi.org/10.1111/gcbb.12141>
- Smith, W.A., Wendt, L.M., Bonner, I.J., Murphy, J.A., 2020. Effects of Storage Moisture Content on Corn Stover Biomass Stability, Composition, and Conversion Efficacy. *Frontiers in Bioengineering and Biotechnology* 8.
- Taheripour, F., Zhao, X., Horridge, M., Farrokhi, F., Tyner, W., 2020. Land Use in Computable General Equilibrium Models. *Journal of Global Economic Analysis* 5, 63–109. <https://doi.org/10.21642/JGEA.050202AF>
- Tahvonen, O., Rautiainen, A., 2017. Economics of forest carbon storage and the additionality principle. *Resource and Energy Economics* 50, 124–134. <https://doi.org/10.1016/j.reseneeco.2017.07.001>
- Wise, M., Calvin, K., Kyle, G.P., Luckow, P., Edmonds, J., 2014. ECONOMIC AND PHYSICAL MODELING OF LAND USE IN GCAM 3.0 AND AN APPLICATION TO AGRICULTURAL PRODUCTIVITY, LAND, AND TERRESTRIAL CARBON. *Climate Change Economics* 5, 1–22.
- Zabel, F., Putzenlechner, B., Mauser, W., 2014. Global Agricultural Land Resources – A High Resolution Suitability Evaluation and Its Perspectives until 2100 under Climate Change Conditions. *PLOS ONE* 9, e107522. <https://doi.org/10.1371/journal.pone.0107522>
- Zhao, X., Calvin, K.V., Wise, M.A., 2020a. The critical role of conversion cost and comparative advantage in modeling agricultural land use change. *Clim. Change Econ.* 11, 2050004. <https://doi.org/10.1142/S2010007820500049>
- Zhao, X., Calvin, K.V., Wise, M.A., Patel, P.L., Snyder, A.C., Waldhoff, S.T., Hejazi, M.I., Edmonds, J.A., 2021. Global agricultural responses to interannual climate and biophysical variability. *Environ. Res. Lett.* 16, 104037. <https://doi.org/10.1088/1748-9326/ac2965>
- Zhao, X., Chepeliev, M., Patel, P., Wise, M., Calvin, K., Narayan, K., Vernon, C., 2024a. gcamfaostat: An R package to prepare, process, and synthesize FAOSTAT data for global agro-economic and multisector dynamic modeling. *Journal of Open Source Software* 9, 6388. <https://doi.org/10.21105/joss.06388>
- Zhao, X., Mignone, B.K., Wise, M.A., McJeon, H.C., 2024b. Trade-offs in land-based carbon removal measures under 1.5 °C and 2 °C futures. *Nat Commun* 15, 2297. <https://doi.org/10.1038/s41467-024-46575-3>
- Zhao, X., van der Mensbrugge, D.Y., Keeney, R.M., Tyner, W.E., 2020b. Improving the way land use change is handled in economic models. *Economic Modelling* 84, 13–26. <https://doi.org/10.1016/j.econmod.2019.03.003>